People`s Democratic Republic of Algeria

Ministry of Higher Education and Scientific Research

University of Echahid Hamma Lakhdar - El Oued

Faculty of Technology

Department of Process Engineering & Petrochemistry

Dissertation

ACADEMIC MASTER

Domain: Science and Technology

Division: Chemical Enginnering

Specialty: Chemical Enginnering

Presented by:

1. **Tedjani Aicha**
2. **Khairani Sara**
3. **Khalifa Hizia**

Entitled:

Effective Remediation of Copper(II) from Aqueous Medium Using A Polymeric Matrix: Optimization via Box-Behnken Design.

Dissertation Submitted in Partial Fulfillment of the Requirements for the Master Degree in Chemical Enginnering

Publicly defended in: ……/…… /2025

Board of Examiners:

Dr. ……..…….	**Chairman**
Dr. Reghioua Abdallah	**Supervisor**
Dr. ……	**Examiner**

Academic Year: 2025/2024

Abstract

The remediation of heavy metals remains a global challenge facing water environmental management amidst the growing demands of industrialization. In this study, Schiff's base chitosan adsorbent has been developed for the efficient removal of Cu^{2+} ions from the aquatic environment. A two-step process: loading with zinc oxide followed by crosslinking with 2-Hydroxy-1,2-Di(phenyl)Ethanone, were performed to synthesize the developed adsorbent, designated as CHI-HDE/ZnO. A batch approach was adopted using Box-Behnken design (BBD) to optimize the highest adsorption capacity of Cu^{2+} ions by CHI-HDE/ZnO under multivariable environments. Surface analysis results revealed that the surface area of CHI-HDE/ZnO (3.762 m^2/g) was multiplied by 5.6 times compared to the original CHI material (0.401 m^2/g). Based on both thermodynamic state functions: Gibbs free energy change ($\Delta G = -3.76, -5.02, -5.54$, and -6.12 kJ $\cdot$ mol^{-1} at 303, 313, 323, and 333 K, respectively), and the Entropy change ($\Delta S = 76.7 J \cdot mol^{-1} \cdot K^{-1}$), the interaction between Cu^{2+} ions toward CHI-HDE/ZnO surface is a spontaneous process, accompanied by heat absorption of 19.0 kJ $\cdot$ mol^{-1}. The pseudo-second-order model well fitted the experimental kinetic data. Furthermore, the CHI-HDE/ZnO adsorbent demonstrated a maximum adsorption capacity of 327.8 mg $\cdot$ g^{-1} for Cu^{2+} ions removal at 323 K, according to the Langmuir isotherm model. These results will offer promising prospects for aquatic environmental organizations, CHI-HDE/ZnO, as a promising adsorbent capable of effectively removing heavy metals, including Cu^{2+} ions, from the aquatic environment.

Keywords: Schiff's base chitosan, Box-Behnken design, Adsorption, Cu^{2+} ions, Isotherm models.

الملخص:

لا يزال معالجة المعادن الثقيلة تحديًا عالميًا يواجه الإدارة البيئية للمياه في ظل الطلب المتزايد للتصنيع. في هذه الدراسة، تم تطوير مادة شيتوزان القائمة على قاعدة شيف كمادة مازة لإزالة أيونات النحاس الثنائي (Cu^{2+}) بكفاءة من البيئة المائية. تم تصنيع المادة المازة المُطورة المُشار إليها باسم CHI-HDE/ZnO عبر عملية من خطوتين: التحميل اكسيد الزنك يليه التشابك مع 2-هيدروكسي-2،1-ثنائي(فينيل) إيثانون. تم اعتماد منهج الدُفعات باستخدام تصميم بوكس-بهنكن (BBD) لتحسين أعلى سعة امتزاز لأيونات Cu^{2+} بواسطة CHI-HDE/ZnO في بيئات متعددة المتغيرات. كشفت نتائج التحليل السطحي أن المساحة السطحية لـ CHI-HDE/ZnO (3.762 م²/غرام) قد تضاعفت بمقدار 5.6 مقارنةً بمادة الشيتوزان الأصلية (0.401 م²/غرام). استنادًا إلى دالتي الحالة الثرموديناميكية: التغير طاقة جيبس الحرة (ΔG=-3.76، -5.02 ،-5.54، و−6.12 كيلوجول/مول عند 303، 313، 323، و333 كلفن على التوالي)، والتغير الإنتروبي (ΔS = 76.7 جول/مول·كلفن)، فإن التداخل بين أيونات Cu^{2+} وسطح CHI-HDE/ZnO كانت عملية تلقائية مصحوبة بامتصاص حراري مقداره 19.0 كيلوجول/ مول. تمثل نموذج الدرجة الثانية الزائف أفضل ملاءمة للبيانات الحركية التجريبية. علاوةً على ذلك، أظهرت المادة المازة CHI-HDE/ZnO سعة امتزاز قصوى بلغت 327.8 ملغ/غرام لإزالة أيونات Cu^{2+} عند 323 كلفن وفقًا لنموذج لانجمير الآيزوثارم. تقدم هذه النتائج آفاقًا واعدة للمنظمات البيئية المائية، حيث تُعتبر CHI-HDE/ZnO مادة مازة واعدة قادرة على إزالة المعادن الثقيلة، بما في ذلك أيونات Cu^{2+}، من البيئة المائية بكفاءة.

الكلمات المفتاحية : شيوزان قاعدة شيف، تصميم بوكس-بهنكن، الامتزاز، أيونات النحاس الثنائي Cu^{2+}، نموذج ايزوثارم.

إهداء

"وقل اعملو سيرى الله عملكم ورسوله والمؤمنين"
الحمدلله والصلاة والسلام على سيدنا محمد صلى الله عليه وسلم.
و الحمدلله الذي يسر لي البدايات واكمل لي النهايات وبلغني الغايات.
ما انتهى درب ولا ختم جهد ولا تم سعي الا بفضل الله فاللهم لك الحمد كما ينبغي لجلال وجهك ولعظيم سلطانك.
اهدي ثمرة هذا العمل الى من كانا لهما الفضل علي ابي و امي سراج دربي بهما ابصرت طريق حياتي واستمددت القوة والعزيمة خلال 17عاما في هذه المسيرة
فهذا العمل ماهو الا ثمرة من ثمرات جهدهم وعطائهم المادي والمعنوي
"وقل ربي ارحمهما كما ربياني صغيرا" .
الى اخوتي واخواتي مصدر فخري وابنائهم وبناتهم وكل من ساهم في العمل .
الى من كان خير عون لي في مسيرتي زوجي الغالي .
الى من ربطني بهم علاقة النسب وعطر الصداقة وورد المحبة.
الى كل من كان له دور في في هذا العمل من طلبة ومعلمين.
فاللهم بارك لي في علمي وعملي واجعلني ممن يستعمل علمه في خدمة دينه ودنياه.

خيراني سارة

إهداء

الحمد لله الذي بنعمته تتم الصالحات في طياتها الكثير من الصعوبات و المشقة والتعب .

اليوم أقطف ثمرها و أهديها الى معلم البشرية أجمعين الهادي الامين محمد صلى الله عليه وسلم.

أهدي ثمرة جهدي المتواضع إلى من وهبوني الحياة الامل و النشأة على الشغف للإطلاع و المعرفة

ومن علموني أن أرتقي سلم الحياة بحكمة وصبر و بر و إحسان و وفاء لهما

إلى من أحمل إسمه بكل إفتخار.. أبي الغالي و إلى معنى الحب والحنان .. امي الحبيبة.

إلى من كانو لي السند في هذه الحياة إخوتي و أخواتي .

إلى كل أهلي و أقاربي إلى كل الأحباب والصديقات .

إلى كل من ساندني من قريب أو بعيد وتمنى لي الخير و النجاح .

إلى كل من وسعه قلبي ولم تسعه أسطري و عباراتي .

أهدي هاذا البحث تعبيرا مني عن خالص شكري لما قدموه لي من دعم معنوي وإعطائي يد العون .

إليكم جميعا أهدي هذا العمل راجية من المولى عز وجل أن يجد القبول والنجاح .

تجاني عائشة

إهداء

الحمدلله والصلاة والسلام على سيدنا محمد المصطفى الأمين.
الحمدلله الذي ماتم جيدا ولا ختم سعي إلا بفضله وما تخطى العبد من عقبات إلا بتوفيقه
بفضل الله اتممت مسيرتي الجامعية.
أهدي ثمرة جهدي ونجاحي المتواضع إلى النور الذي أضاء دربي إلى معلمي الأول الرجل الذي سعى طوال حياته لأكون الأفضل أبي الغالي .
إلى من كانت الداعم الأول للتحقيق طموحي إلى من كانت ملجأي ويدي اليمنى في هذه المرحلة إلى من أبصرت بها طريق حياتي وأعتزازي بذاتي
إلى القلب الحنون إلى من كانت دعواتها تحيطني أمي الحبيبة .
إلى من وهبني الله نعمة وجودهم في حياتي إلى العقد المتين من كانوا عونا لي في رحلة بحثي إخواني وأخواتي.
إلى كل أهلي وأقاربي من الأجداد إلى الأحفاد إلى كل الأحباب و الصديقات .
ثم إلى كل طالب علم سعى بعلمه ليفيد الأسلام و المسلمين بكل ما أعطاه الله من علم ومعرفة .
وأخيرا إلى كل من ساعدني و كان له دور من قريب أو بعيد في أتمام هذه الدراسة
سائلة المولى عز وجل أن يجزي الجميع خير جزاء في الدنيا و الأخرة.

خليفة حيزية

ACKNOWLEDGEMENTS

First and foremost, we would like to express our deepest gratitude to ALLAH (s.w.t) for granting us perseverance and patience throughout this Master's journey.

We are profoundly grateful to Dr. Reghioua Abdallah for his unwavering support and timely corrections when we needed them most during our research.

We would also like to extend our sincere thanks to Dr. ....., and Dr. ..... for agreeing to discuss our thesis and provide invaluable feedback.

Lastly, but certainly not least, we are immensely thankful to our family for their unwavering support. Thank you for always being there for us and offering your help whenever we needed them. .

CONTENTS

LIST OF TABLES

LIST OF FIGURES

LIST OF Abbreviations

RSM	Response Surface Methodology
BBD	Box Behnken design
SEM	Scanning electron microscope
EDX	Energy- dispersive x-ray spectroscopy
FTIR	Fourier Transform Infrared
Qmax	Maximum adsorption capacity
q_e	Adsorption capacity at equilibrium
q_t	Amount of adsorbed at time
R^2	Correlation coefficient
K_L	Langmuir constant
K_f	Freundlich constant
K_T	Temkin constant
C_0	Beginning concentration
C_e	Equilibrium concentration
t	adsorption time
V	Volume of adsorbate
W	Weight of adsorbent
PFO	pseudo-first-order
PSO	pseudo-second-order
CHI	Chitosan
HDE	2-Hydroxy-1,2-Di(phenyl) Ethanone

CHAPTER 1

GENERAL INTRODUCTION

1.1 Background of the study

The survival of humanity on Earth depends on three essential resources: water, air, and soil. Water is considered the most important of these resources, as it forms the fundamental medium for the emergence and continuation of life. Water is described as "the most common and least understood solvent" due to its unique physical and chemical properties that have allowed life to evolve within it. As Szent-Györgyi stated, "There is no doubt that water operates in multiple ways within the cell. Life originated in water, and it thrives in it as its solvent and medium. It is the foundation of life". All biological reactions occur in water, making its pollution a major concern when it affects living systems [3].

Heavy metal pollution of water sources has emerged as one of the serious global environmental challenges, threatening both aquatic ecosystems and human health. This pollution is exacerbated by industrialization, climate change, and urbanization. Sources of pollution include mining waste, landfill leachate, and municipal and industrial wastewater. Heavy metals, especially certain types, have lethal effects on all forms of life even at low concentrations [4].Among the environmentally polluting heavy metals is copper (Cu^{2+}), which is one of the important engineering materials with wide industrial applications. It is considered one of the oldest known toxic metals and is used as a raw material in many industries.

In recent decades, various methods for purifying contaminated water have been studied, including chemical precipitation, nanofiltration, solvent extraction, ion exchange, and adsorption. Among these methods, adsorption technology has garnered significant scientific interest due to its high efficiency, low cost, ease of handling, and the availability of various adsorbent materials [5].

The adsorption process is considered a promising and versatile method for removing toxic heavy metals from water. This process involves transferring pollutants from an aqueous solution to the surface of a porous solid material known as the adsorbent. This occurs due to attractive forces between the pollutants (such as heavy metals) and the surface of the adsorbent, which may involve chemical bonds or physical forces. These interactions depend on the functional groups present on the adsorbent surface, its porous structure, and the nature of the pollutants[6].

Many global research studies in recent years have focused on natural polymers and methods to enhance their ability to bind with metals. The adsorption process depends on various experimental conditions, such as particle size, pH, metal concentration, ligand concentration, and ion competition. Scientists have directed their efforts towards finding low-cost and read-

ily available biomaterials for wastewater treatment. Among the natural polymers that have received significant attention in this field are chitosan, alginates, cellulose, and lignin [5].

The ideal adsorbent material for removing heavy metal ions possesses several characteristics, including a large surface area, high adsorption capacity, suitable pore size, mechanical stability, environmental compatibility, ease of access, regenerability, cost-effectiveness, and high selectivity. Therefore, some recent studies have focused on developing polymeric materials such as chitosan and its derivatives. Chitosan is an abundant biopolymer derived from the alkaline deacetylation of chitin. It exhibits high adsorption capacity for heavy metal ions compared to some conventional adsorbents due to the presence of reactive hydroxyl (-OH) and amino (-NH2) groups. However, chitosan has some limitations, such as low stability in acidic environments, insufficient mechanical strength, and low thermal stability, which restrict its applications. As a result, researchers have introduced physical and chemical modifications to enhance its adsorption properties [7].

In this context, this research aims to explore the possibility of using modified chitosan as an adsorbent to remove copper Cu^{2+} from contaminated water. Copper was chosen as a model for heavy metals due to its wide industrial significance and its toxic impact on the environment and living organisms.

1.2 Problem statement

The rapid pace of industrial development has led to an increase in the amount of waste being unregulatedly discharged into water bodies, contributing to the pollution of water resources, particularly heavy metals. This pollution poses a significant risk to current and future generations, imposing significant health and environmental burdens. Recently, adsorption technology has emerged as an effective and low-cost method for removing these heavy metals from liquid waste. This technology uses biomaterials extracted from natural waste, such as chitosan, due to their biodegradability, widespread availability, and low cost.

Chitosan has recently attracted the attention of many researchers as a promising adsorbent for the removal of pollutants, including both organic and inorganic pollutants. However, this unmodified adsorbent still suffers from some limitations, such as its solubility in acidic media, low surface area, and thermal resistance. It also has a tendency to shrink and deform after drying.

Research Question:

How effective is zinc oxide-modified chitosan in adsorbing copper ions laden in aqueous solution?

1.3 Objectives

There are numerous adsorbents, such as clay, activated carbon, and chitosan, which have been previously used to remove pollutants from aqueous solutions [8; 9]. However, the use of chitosan as an adsorbent in wastewater treatment has some limitations, such as low surface area, solubility in many organic acids, poor mechanical strength, and chemical stability [10]. In general, several methods can be used to improve the properties of chitosan, firstly: physical modification, such as the incorporation or addition of some metal oxides into the chitosan matrix. Secondly, chemical modification, such as chemical bonding reactions. Therefore, the main objectives of the current study are:

✍ **a.** To prepare zinc oxide from zinc acetate dihydrate via the solution-dropping technique.

✍ **b.** To prepare Schiffs base Chitosan via loading ZnO into chitosan (CHI) matrix, followed by using 2-Hydroxy-1,2-Di(phenyl) Ethanone as a cross-linking agent.

✍ **c.** To characterize CHI-HDE/ZnO composites by scanning electron microscopy (SEM), Fourier transform infrared spectroscopy (FTIR), and Brunauer-Emmett-Teller (BET) analysis.

✍ **d.** To adopt the batch adsorption tests for the removal of Cu^{2+} ions from aqueous solution by response surface methodology (RSM).

✍ **e.** To optimize the key variables conditions for the Cu^{2+} adsorption process by box behnken design (BBD).

1.4 Significance of study

The following are the significances of this study:

i. Copper is a heavy metal classified as a toxic pollutant, especially for living organisms. Therefore, finding an effective method for removing Cu^{2+} ions from aquatic medium is of paramount importance.

ii. Adsorption using biopolymer-derived adsorbents is a cost-effective and energy-efficient technology, and is less hazardous than chemical treatment methods, making it an effective and environmentally friendly approach.

iii. Application of an effective method to investigate the optimal removal efficiency of copper ions from aqueous medium and under different environmental conditions, using a simulation approach design.

iv. This research will act as a blueprint for the removal of Cu^{2+} ions laden in water using CHI-HDE/ZnO composite, even at high concentrations.

1.5 Thesis Layout

This thesis is divided into four chapters. Chapter one presents the general introduction, which contains: background of the study, problem statement, objectives, and significance of the study.

The literature review was outlined in Chapter Two, which focused on a general study of water pollutants and methods of treatment, with particular emphasis on the adsorption process.

Chapter Three presents the methodology and procedures followed for the removal of Cu^{2+} ions from aqueous medium. This methodology involves four parts: a description of the chemicals used, the preparation method for both adsorbent and adsorbate, characterizations, and simulated analysis adopted using Response Surface Methodology (RSM).

Chapter Four discusses the research findings. Starting with characterization of the prepared adsorbent, followed by its evaluation through statistical analysis, as well as various adsorption studies.

CHAPTER 2

LITERATURE REVIEW

2.1 Introduction

God Almighty endowed water with distinctive physical, chemical, and biological properties, making it the foundation upon which the survival of living beings depends. Water is considered the most magnificent and essential of liquids, as life on Earth would be unimaginable without it. Moreover, God created the heavens and the Earth and granted humanity the ability to live in them, bestowing upon them this precious resource that forms the core of their existence and that of all other creatures.

The rapid pace of industrialization in developing countries, coupled with the enormous and ever-increasing demand for heavy metals, results in the emission of large quantities of these pollutants from human sources into the biosphere. Consequently, a serious problem has[11; 12] emerged in modern times pollution, which has become one of the greatest challenges facing humanity today .

2.2 Water

Freshwater is considered one of the most precious gifts bestowed upon our planet, playing a crucial role in sustaining human life and supporting a diverse array of living organisms [13]. However, this limited natural resource faces significant threats from contaminants resulting from modern agricultural and industrial practices. The problem is exacerbated by the continual increase in the discharge of industrial wastewater and sewage into rivers and adjacent lands, driven by the growing demand for food and housing. According to the NORMAN Network report [14], water bodies now contain numerous toxic substances, including agricultural chemicals, heavy metals, oil derivatives, and synthetic dyes. It is clear that these unsustainable practices will impose a heavy burden on both current and future generations, as global pollution levels are expected to continue rising with potentially severe consequences. In fact, the United Nations World Water Assessment Program (WWAP) predicts that global water demand will increase by more than 55 % over the next two decades.

Among the essential parameters for assessing water quality, Chemical Oxygen Demand (COD) plays a pivotal role, as it measures the amount of oxygen required to oxidize both organic and inorganic substances in water. Elevated COD values indicate severe pollution [15], revealing the presence of pollutants that consume the oxygen necessary for the survival of aquatic organisms. The entry of organic mattersuch as that found in wastewater, industrial effluents, and agricultural runoffraises COD levels, leading to oxygen depletion and creating low-oxygen conditions that can result in the death of fish and other organisms. Consequently,

regular monitoring of COD is crucial for identifying and managing sources of pollution, thereby contributing to the protection of aquatic ecosystems and human health. Effective wastewater treatment and pollution control strategies are essential steps for reducing COD levels and preserving water quality.

2.3 Water pollutant

Water pollution, also known as aquatic pollution, refers to the contamination of water sources with harmful substances that negatively affect their usability. This type of pollution is mainly due to human activities. As a result, water bodies such as lakes, rivers, oceans, reservoirs, ponds, and groundwater become contaminated when these dangerous materials mix with them.

Among the main sources contributing to water pollution are the discharge of sewage, as well as industrial, agricultural, and urban runoff, including stormwater. Both surface and groundwater are affected by this contamination.

Water pollution causes numerous negative effects; it weakens aquatic ecosystems, contributes to the spread of waterborne diseases when polluted water is used for drinking or irrigation, and diminishes the environments ability to provide clean drinking water[16].

2.3.1 Sources of water pollution

There are a variety of sources from which water pollution arises, and in this section, we will limit ourselves to mentioning some of them:

2.3.1.1 Thermal Pollution

Thermal pollution occurs when water temperatures rise as a result of human activities, such as industrial discharge or power plant cooling processes, leading to damage to aquatic organisms and disruptions in ecosystems. Oxygen depletion pollution arises when pollutants like organic waste or an excess of nutrients cause a decline in dissolved oxygen levels in the water, creating a harmful environment for fish and other aquatic life. To combat water pollution, it is essential to identify its sources and implement effective measures to protect our water resources. By addressing these various types of pollution, we can improve water quality and preserve our environment [17].

2.3.1.2 Agricultural Activities

Agricultural practices significantly contribute to water pollution through the use of fertilizers and pesticides in crop cultivation. When applied, these chemicals can infiltrate the soil, leading to groundwater contamination. Additionally, water runoff during rainfall carries these pollutants to adjacent water bodies, resulting in nutrient buildup, excessive algal growth, and the deterioration of aquatic ecosystems. Moreover, the presence of pesticides in water sources poses a risk to human health and wildlife. Overall, surface runoff from agricultural activities is considered one of the primary sources of water pollution [18] .

2.3.1.3 Wastewater discharges

The discharge of wastewater is a major factor in water pollution, resulting from various human activities such as domestic, industrial, and agricultural uses. Domestic wastewater contains liquid waste from households and sewage, which may carry harmful bacteria and polluting chemicals. Industrial waste, discharged from factories and facilities, may include toxic compounds such as heavy metals, solvents, and hazardous chemicals. Additionally, surface runoff from agricultural activities transports pesticides, fertilizers, and animal waste into water sources, leading to contamination. These pollutants negatively affect water quality, harm aquatic ecosystems, and pose a threat to human health. Therefore, implementing effective solutions for wastewater treatment and management is essential to mitigate these issues and ensure the availability of clean and safe water [19] .

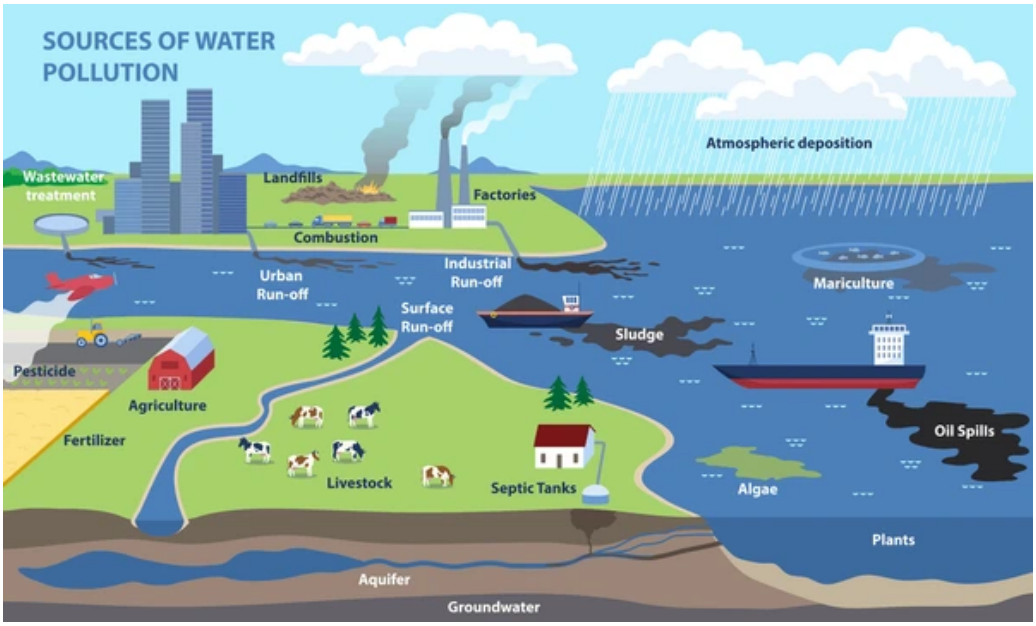

Figure 2.1: Sources of water pollutant

2.3.1.4 Heavy Metals

✍ a. Definition of Heavy Metals

Heavy metals are a heterogeneous group of elements that differ in their functions and chemical properties. They primarily belong to the transition elements in the periodic table,It is defined as the elements that have a density greater than 5 g/cm^3, or those with an atomic number exceeding 20 .

These metals include elements such as iron (Fe), lead (Pb), and copper (Cu), which occur naturally in the Earth's crust. Despite their importance in certain biological and industrial processes, their accumulation at high concentrations can have negative effects on the environment and health. Heavy metals have the ability to bioaccumulate in living organisms, which can cause toxic effects, whether acute or chronic[20].

Essential metals maintain the metabolic processes of the human body. For example, copper is essential for hemoglobin formation and carbohydrate metabolism. However, when present in excess amounts, they can cause cellular damage [21].

✍ b. Classification of Heavy Metals

The metals present in the environment can be classified into essential metals and toxic metals.

✍ b - 1 Essential Heavy Metals

These are the metals necessary for living organisms and cannot be dispensed with, as they participate in many cellular processes such as metabolic reactions or enzymatic reactions. They are found in very small amounts in biological tissues and may become toxic when their concentration exceeds a certain threshold. This is the case for copper (Cu), zinc (Zn), and iron (Fe).

✍ b - 2 Toxic Heavy Metals

They have a polluting nature and toxic effects on living organisms even at low concentrations, and they have no benefit to the cell. This is the case for lead (Pb), mercury (Hg), and cadmium (Cd).

Figure 2.2: Heavy Metals

✍ c. Toxicity of Heavy Metal

Heavy metals are characterized by their non-biodegradable properties, allowing them to gradually accumulate in living tissues. They are also characterized by their environmental persistence, enabling them to directly or indirectly affect many living organisms.

Due to the discharge of large quantities of industrial wastewater contaminated with metals, industries that utilize heavy metals such as chromium (Cr), copper (Cu), and arsenic (As) are among the most hazardous chemical industries [22]. Because of their high solubility in aquatic environments, living organisms can easily absorb heavy metals. When these metals enter the food chain, they can accumulate in high concentrations within the human body, potentially leading to serious health disorders when permissible levels are exceeded. On the other hand, heavy metals expose aquatic organisms such as phytoplankton, zooplankton, and fish to acute and chronic toxic effects. They accumulate in their tissues, causing oxidative stress due to the formation of free radicals, endocrine disruption, and damage to vital organs such as the liver and kidneys [23].

Table 2.1: Types of heavy metals and their impact on human health with permissible limits [1]

Pollutants	**Major sources**	**Effect on human health**	**Permissible level ($mg{\cdot}L^{-1}$)**
Cadmium	*Welding, electroplating, pesticides, fertilizers, Cd and Ni batteries*	Renal dysfunction, lung disease, lung cancer, increased blood pressure, kidney damage, bronchitis, gastrointestinal disorders	0.06
Mercury	*Pesticides, batteries, paper industry*	Tremors, gingivitis, minor psychological changes, acrodynia (pink hands and feet), spontaneous abortion, protoplasm poisoning	0.01
Copper	*Mining, pesticide production, chemical industry, metal piping*	Anemia, liver and kidney damage, stomach and intestinal irritation	0.1

✍ d. Sources of Heavy Metals

Heavy metals originate from both natural and human-made sources, contributing to the pollution of vast areas worldwide. Since these metals are naturally found in the Earth's crust, their presence in the soil results from weathering processes.

✍ d - 1 Natural Sources

Geological parent rocks and rock formations are the primary natural sources of heavy metals. Their concentration and composition depend on the type of rocks and surrounding environmental conditions. Volcanic eruptions release large amounts of heavy metals along with toxic gases, while forest and grassland fires contribute to their emission into the air. Additionally, natural vegetation introduces heavy metals into the soil and atmosphere through leaf and stem leaching, decomposition, and volatilization [24].

✍ d - 2 Agricultural Sources

Organic and inorganic fertilizers are among the most significant sources of heavy metals in agricultural soils. These include lime, sewage sludge, irrigation water, and pesticides, particularly fungicides. Studies indicate that continuous irrigation can lead to the accumulation of elements such as lead (Pb) and cadmium (Cd) in the soil, as irrigation water sources such as deep wells, rivers, lakes, and canals may contain these metals[25].

✍ d - 3 Industrial Sources

Industrial sources of heavy metals include mining and refining processes, where emissions

vary depending on the type of mining, leading to direct or indirect contamination of surrounding soils. Pollution can also occur through surface runoff from mining waste, dust from ore transportation, and metal corrosion.

Other industrial sources include power plants, plastic manufacturing, textiles, microelectronics, wood processing, and paper production. Additionally, waste incineration, landfills, and transportation play a significant role in the spread of heavy metals in the environment [26].

✍ e. Types of Metals

✍ e - 1 Cadmium

∗ Cadmium is a chemical element with a silvery-white color, soft and malleable, with the atomic number 48. It is classified in group 12 of the periodic table, discovered by German chemist F. Stromeyer in 1817 as an element of smithsonite (ZnCO3) present in zinc ore. Cadmium is characterized by its electronic configuration [Kr] 4d10 5s2. It exists at a concentration of 0.15 parts per million in the Earth's crust, and the most common cadmium mineral is greenockite (CdS). Cadmium is recovered as a byproduct from sulfide deposits, which mainly contain lead, zinc, and copper. Cadmium is considered harmful to the environment and humans, as it can cause serious health problems when exposed to it at low concentrations [27].

∗ Cadmium is considered a toxic and hazardous metal to human and animal health, acting as a stimulator of cell division and enhancing cancer growth in many tissues, as well as stimulating cell division. On the other hand, it leads to cell death, resulting in tissue damage in the kidneys.

✍ e - 2 Mercury

∗Mercury is a chemical element with the symbol Hg and atomic number 80. It is a heavy metal with a silver-white color, low viscosity, and can exist in a liquid state at room temperature. Mercury can exist in various chemical forms, including metallic mercury (Hg), mercurous mercury (Hg2+), mercuric mercury (Hg22+), and organic mercury compounds (such as methylmercury). The use of mercury is considered hazardous to the environment and public health, and therefore its use and storage are strictly controlled in many countries.

∗Mercury is a toxic heavy metal that affects cells in various ways. Exposure to mercury vapor causes inflammation in the respiratory system and neurological dysfunction. Mercury salt poisoning causes inflammation in the abdomen and kidneys, as well as renal tubular necrosis. It may also lead to immune disorders, neurological damage, and kidney and brain dysfunction, and can be fatal. Mercury should be handled with caution due to its toxicity[28].

✍ e - 3 Manganese

Manganese exists in Its pure form as a silvery-gray metal. It is hard but very brittle and prone to fracture. Magnesium loses its luster when exposed to oxygen. Manganese can exist In different chemical forms, such as :

- Manganese(II) oxide MnO
- Manganese(III) oxide Mn_2O_3
- Manganese dioxide MnO_2

Magnesium is present in all tissues of the body because it is essential for many important enzymatic reactions, such as the synthesis of amino acids, lipids, proteins, and carbohydrates. In some cases, magnesium may accumulate in certain areas of the brain after exposure to high levels, which can lead to magnesium-induced neurotoxicity, medically known as magnesia intoxication[29]. This toxicity usually manifests as a movement disorder similar to Parkinson's disease. However, the detailed mechanisms of magnesium neurotoxicity are not yet fully understood .

✍ f - 3 Copper

Copper is a chemical element of great significance in technology, particularly in electrical technology, due to its high ability to conduct electricity and heat. Copper is a typical transition metal that is widely distributed in nature at low concentrations. It is found in the Earth's crust, copper ores, and other deposits. It is the third most used metal in the world and belongs to the group of heavy metals. Copper is generally considered a highly hazardous heavy metal, yet it is also an essential element for humans, playing a vital role in enzyme synthesis, bone formation, and tissue development. The different forms of copper include metallic copper Cu(0), monovalent copper ion Cu(I) (cuprous ion), and divalent copper ion Cu^{2+} (cupric ion), with Cu^{2+} being the most toxic and most prevalent form in the environment [30].

✍ f - 3 - 1 Properties of Copper

The main properties of copper include high electrical and thermal conductivity, corrosion resistance, ductility, malleability, and high strength. Furthermore, copper is distinguished by its attractive color, non-magnetic nature, and ease of finishing with coatings or polishing. It can be welded and soldered efficiently. Some of these properties can be enhanced by alloying copper with other metals, leading to the development of well-known alloys such as brass, bronze, copper-nickel alloys, and nickel silver.

- Atomic number: 29
- Atomic weight: 63.54
- Group: IB in the periodic
- table : following silver (Ag) and gold (Au).
- Electronic configuration: 2:8:18:1

✍ f - 3 - 1 - 1 Chemical Properties

When exposed to air, copper forms a thin layer of copper(II) oxide (CuO) on its surface, which has a dark red color. When heated, it reacts with oxygen to produce copper(I) oxide (Cu_2O)at high temperatures.

In humid environments or upon contact with carbon dioxide or sulfur dioxide, a green patina forms on its surface, consisting of basic copper carbonate and basic copper sulfate.

Copper reacts with halogens such as chlorine and bromine but does not dissolve in non-oxidizing acids in the absence of oxygen. However, it readily dissolves in oxidizing acids like nitric acid (HNO_3) and sulfuric acid (H_2SO_4), as well as in alkaline solutions such as ammonia (NH_3) or potassium cyanide (KCN) [31].

Copper exhibits oxidation states ranging from -1 to +4, with the most common being Cu (metallic copper), Cu^+ (cuprous ion), and Cu^{2+} (cupric ion). Due to its standard reduction potential of 0.340 V, it is considered a noble metal with relative resistance to corrosion.

Copper forms divalent salts, whereas gold is more stable in forming trivalent compounds. When copper loses its outer electron, it becomes aCu^+ ion, and upon losing an additional electron, it forms a Cu^{2+} ion, influencing its chemical stability and corrosion behavior [32].

✍ f - 3 - 1 - 2 Physical Properties

Copper is one of the rare metals that naturally exhibits a rich color, alongside gold, unlike most metals that appear in shades of gray. Its distinctive red hue becomes particularly visible when freshly cut or polished.

Solid copper has a bright metallic luster, but it quickly tarnishes upon exposure to air.

Beyond its striking appearance, copper is known for its high ductility and malleability, making it easily shapeable. It crystallizes in a face-centered cubic (fcc) structure, with its crystals classified within the Fm-3m space group.

Copper is widely used in alloy formation, such as bronze and brass, and can be fully blended with gold. It is also among the best conductors of heat and electricity, second only to pure silver [31].

✍ f - 3 - 2 Thermal constants of copper

- Melting point: 1083.0°C (1981.4°F)
- Boiling point: 2595°C (4703°F)
- Latent heat of fusion: 49.8 cal/gram (89.8 Btu/lb)
- Heat capacity: 0.0919 cal/gram/°C
- Linear thermal expansion coefficient: $16.42 * 10^{-6}$/°C
- Thermal conductivity at 18°C: 0.934 cal/cm/cm^2/sec/°C[32]

✍ f - 3 - 3 Copper toxicity

Copper is an essential trace element that contributes to maintaining the health balance of the body and mind. However, when its levels exceed the natural threshold required for living organisms, it can accumulate and cause permanent damage [33]. Due to its non-biodegradable nature, copper is classified as a potentially toxic substance when it accumulates in the environment .

Recently, cases of copper poisoning have increased due to exposure through inhalation, consumption of contaminated food and water, or skin contact with copper-containing sources. Food and water are the primary sources of copper absorption, although small amounts can also enter the body through inhalation or direct contact.

Copper possesses an electronic structure that enables it to interact directly with oxygen, allowing it to act as a catalyst in numerous oxidation-reduction reactions. Its ions play a pivotal role in cellular respiration, protection against oxidation, regulation of neurotransmitter activity, and the formation of connective tissues. However, the very properties that make copper biologically beneficial also make it potentially toxic [34].

The human body contains copper at levels ranging between 0.1 and 10 mg per 100 grams of wet tissue or bodily fluids. Its binding to specialized proteins and amino acids serves as a protective mechanism to limit oxidative damage. However, under conditions of oxidative stress, an increase in reactive oxygen species (ROS) can damage vital components such as lipoproteins,

membranes, and cells. In such cases, copper ions bound to proteins are released and become active in oxidation-reduction processes. Although the binding of copper to proteins limits its oxidative reactions, it is not an absolute protective mechanism [35].

2.4 Adsorption

Over the past years, many technologies and methods have been developed to remove pollutants from water sources, including: sedimentation, ion exchange, biological and physical treatments, and adsorption. The term adsorption first appeared in 1881 by the scientist Kaiser to distinguish it from the phenomenon of absorption.

The applications of this phenomenon have evolved to become a fundamental pillar in water purification and industrial waste treatment processes, especially in removing organic pollutants. Their effectiveness is not limited to this field but extends to air purification and toxic waste management.

2.4.1 Definiton of adsorption

Adsorption is a physicochemical process in which a gaseous or liquid substance accumulates on the surface of a solid material upon contact. The adsorbed substances are attracted to the atoms of the solid surface, making adsorption an effective method for removing toxic compounds from the environment.

Materials used in adsorption are characterized by a fine structure with small pores, which increases their active surface area per unit mass, enhancing their absorption efficiency. The surface where adsorption occurs is called the adsorbent , while the substance accumulated on it is known as the adsorbate . The adsorbed molecules bind to active sites through van der Waals forces.

Adsorption plays a fundamental role in physical, biological, and chemical processes, contributing to air pollution reduction and the purification of water from harmful heavy metals.

Adsorption can occur between solid and liquid, liquid and liquid, gas and liquid, or gas and solid. It can be monomolecular, forming a single layer, or multimolecular, involving the accumulation of multiple layers on the adsorbent surface [36].

2.4.1.1 physisorption

It is a process in which molecules are fixed onto the surface of a solid material through weak van der Waals forces, without forming chemical bonds. It is characterized by rapid occurrence, reversibility (ability to be removed by changing conditions such as pressure or temperature), and the possibility of forming multiple layers due to its non-selectivity for specific sites on the surface. This phenomenon relies on low-energy electrostatic interactions (less than 20 kJ/mol),

making it suitable for applications like gas storage or purification, where it can be easily reversed without causing chemical changes to the adsorbed material or the surface [36].

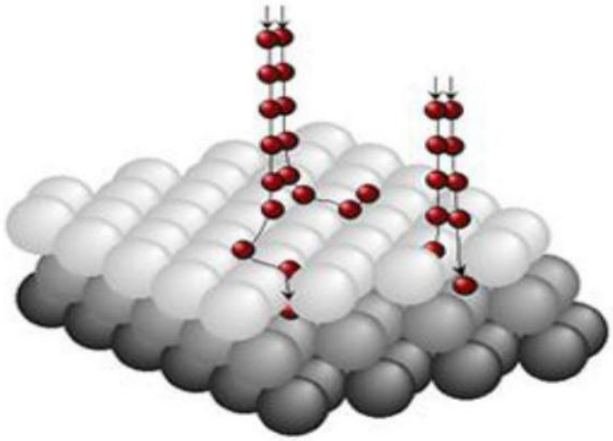

Figure 2.3: physical adsorption

2.4.1.2 chemisorption

It is a process in which molecules or ions are fixed onto the surface of a solid material through the formation of strong chemical bonds (covalent or ionic), accompanied by electron exchange between the adsorbed substance and the surface, making it selective and often irreversible [36]. It is characterized by the formation of a single layer due to the saturation of adsorption sites and is associated with high energies (above 100 kJ/mol) that may alter material properties or dissociate them, unlike weak and reversible physisorption. This phenomenon is used in applications such as chemical catalysis, where molecules are activated through interaction with the surface[37].

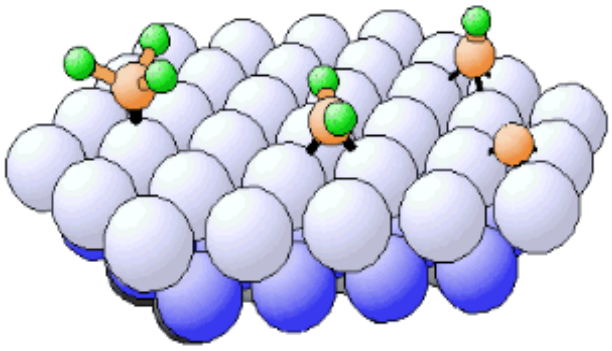

Figure 2.4: Chemical adsorption

The following Table: 2.2 shows the difference between chemisorption and Physisorption.

Table 2.2: The difference between chemisorption and Physisorption

Properties	**Chemisorption**	**Physisorption**
bonding type	chemical bonds	van der Waals bond
layer kind	mono layer	mono, or multi layers
	slowly and irreversibly	rapid and reversibly
adsorption heat	more than 10 K Cal/mol	less than 10 KCal/mol
	needs to an activation energy	does not need to an activation energy

2.4.2 The Factors Influencing Adsorption

Several key factors influence the effectiveness of the adsorption process, including the amount of adsorbent, pH, adsorption time, temperature, and the beginning concentration. Optimizing these factors is essential for developing an industrial-scale heavy metal removal treatment process. The next section will discuss these factors [38].

2.4.2.1 The amount of adsorbent

The amount or dosage of an adsorbent is a critical factor in the efficiency of the adsorption process. Firstly, Increasing the dosage enhances adsorption due to the availability of a greater number of active sites on the surface. However, exceeding the optimal dosage can lead to decreased performance as the sites become saturated and the concentration gradient between the adsorbate and adsorbent decreases [37].

The dosage determines the adsorption capacity of the material under operating conditions, as higher dosages are generally associated with improved pollutant removal rates. Optimizing the adsorbent dosage is essential to achieve maximum adsorption efficiency with minimal adsorbent usage, contributing to cost reduction and ensuring the feasibility of large-scale industrial applications [39].

2.4.2.2 PH

The pH level is a pivotal factor in the performance of adsorbents in water treatment, as it determines the ionization level of molecules and the surface properties affecting adsorption

efficiency. pH surpasses other factors in its influence by controlling the distribution of surface charges during ionic interactions [40].

2.4.2.3 Adsorption time

The efficiency of the adsorption process is directly proportional to the adsorption time, as increasing the reaction duration leads to a more complete process. However, this extension requires designing equipment with larger operating capacities. On the other hand, prolonged contact periods contribute to reducing the resistance of the boundary layer, which enhances the transfer of metal molecules to active sites and significantly increases the adsorption rate.

2.4.2.4 The temperature

The increase in temperature enhances the adsorption rate by expanding the surface area and the pores of the adsorbent. Temperature is an important physico-chemical factor, as it can influence the adsorption capacity of the adsorbent. If adsorption increases with rising temperature, the process is endothermic. This increase may be attributed to the availability of more active sites on the surface of the adsorbent [41].

Conversely, if the adsorption capacity decreases with increasing temperature, the process is exothermic. This decrease may occur because higher temperatures weaken the adsorptive forces between the adsorbate molecules and the active sites on the adsorbent, leading to reduced adsorption [40].

2.4.2.5 Beginning Concentration

The beginning concentration of metal ions can influence their removal efficiency, as factors such as the availability of active binding sites on surfaces and their ability to form chemical bonds with the ions play a crucial role. The initial concentration of the solution can provide a significant driving force to overcome mass transfer resistance of the metal between the liquid and solid phases. An increase in concentration acts as a natural catalyst, accelerating chemical reactions or adsorption processes, thereby ensuring more effective removal of heavy metals or targeted ions [39].

2.4.3 Adsorption kinetics

Adsorption kinetics are studied by monitoring the change in the amount of adsorbate over time and the time required to achieve adsorption equilibrium. Adsorption kinetics describe the

rate at which the solute transfers from the solution to the surface of the adsorbent, contributing to the understanding of the adsorption mechanism and the transfer process between the liquid and solid phases. This understanding has led to the development of kinetic properties and the use of various models to analyze adsorption kinetics and understand the nature of interactions at the liquid-solid interface [42].

Two types of adsorption kinetics can be distinguished: pseudo-first-order (PFO), pseudo-second-order (PSO).

2.4.3.1 PFO

The pseudo-first-order kinetic model is commonly used to simulate the adsorption behavior of materials over time. This model assumes a direct proportional relationship between the rate of temporal change in the adsorption of the adsorbed substance and the difference in concentration between the current state of the solute and the saturation state [43]. The rate constant for adsorption is determined using the pseudo-first-order equation, as described by. equations: 2.1 :

$$q_t = q_e \left(1 - \exp(-K_1 t)\right) \tag{2.1}$$

Where:

q_t: The amount of adsorbate at time t and its unit $(\mathrm{mg} \cdot \mathrm{g}^{-1})$

q_e: Adsorption capacity at equilibrium per gram of adsorbent $(\mathrm{mg} \cdot \mathrm{g}^{-1})$

K_1: the rate constant of adsorption $(min^1\ )$

2.4.3.2 PSO

In studies of the interactions between metal ions and functional groups, McKay introduced in 1999 the concept of the pseudo-second-order kinetic model, also known as the pseudo-second-order kinetics model [44]. This model is represented by the following equations: 2.2 :

$$q_t = \frac{t}{(\frac{1}{K_2 q_e^2}) + (\frac{t}{q_e})} \tag{2.2}$$

Where:

K_2: The rate constant of adsorption for the second-order pseudo-dynamic model (min $\mathrm{mg} \cdot \mathrm{g}^{-1}$)

2.4.4 Adsorption models

2.4.4.1 Langmuir model

The Langmuir adsorption model was initially developed to describe the process of gas adsorption on solid surfaces. This empirical model is based on the assumption that adsorption occurs in a single layer at homogeneous sites on the adsorbent surface, which is why it is commonly referred to as homogeneous adsorption [45]. The Langmuir isotherm model can be expressed in both linear and nonlinear forms, as shown in equations: 2.3 , and 2.4.

$$\frac{1}{q_e} = \frac{1}{q_{max}} + \frac{1}{q_{max} K_L} \cdot \frac{1}{C_e} \tag{2.3}$$

$$q_e = \frac{C_e}{\frac{1}{q_{max} K_L} + \frac{C_e}{q_{max}}} \tag{2.4}$$

Where :

q_{max}: The maximum adsorption capacity ($\mathrm{mg \cdot g^{-1}}$)

q_e: the amount of adsorbate at equilibrium ($\mathrm{mg \cdot g^{-1}}$)

C_e:equilibrium concentration of the adsorbate ($\mathrm{mg \cdot L^{-1}}$)

K_L: Langmuir constant ($\mathrm{L \cdot mg^{-1}}$)

2.4.4.2 Freundlich model

The Freundlich model is one of the oldest models used to describe non-ideal and reversible adsorption. This empirical model describes multilayer adsorption that occurs on a heterogeneous surface, where the heat of adsorption and the tendency of molecules to bind to the adsorbent vary . The model is based on the assumption of varying surface energies, making it widely applicable in heterogeneous systems, particularly when dealing with organic compounds or highly reactive substances on molecular sieves and adsorbents [46]. The Freundlich isotherm model can be expressed in both nonlinear and nonlinear forms, as shown in equations: 2.5 , : 2.6

$$q_e = K_f C_e^{1/n} \tag{2.5}$$

$$\log q_e = \log K_f + \frac{1}{n} \log C_e \tag{2.6}$$

Where :

q_e: The amount of adsorbed material ($mg \cdot g^{-1}$)

K_f, n are constants of Freundlich

C_e: equilibrium concentration of the adsorbate ($mg \cdot L^{-1}$)

2.4.4.3 Temkin model

This model is based on the facilitating temperature, assuming that an increase in the rate of solid surface recovery leads to a linear decrease in the heat of adsorption. It was later developed into a facilitating equation for gas adsorption on solid materials and subsequently applied to the liquid phase [47]. The model is expressed by the following nonlinear equation 2.7 :

$$q_e = \frac{RT}{b_T} ln(K_T C_e) \tag{2.7}$$

Where :

q_e: Equilibrium amount adsorbed ($mg \cdot g^{-1}$)

T: Temperature (k)

R: Gas constant ($j \cdot mol^{-1} \cdot K^{-1}$)

C_e:Equilibrium adsorption concentration ($mg \cdot L^{-1}$)

b_T and K_T : Characteristic constants of the adsorbent/adsorbate system ($j \cdot mol^{-1}$) , and ($L \cdot g^{-1}$), respectively.

2.5 Chitosan

Chitosan is derived from chitin (the second most abundant natural polymer after cellulose) through the partial removal of acetyl groups, making it soluble in acids. Chitin is a natural polymer found in marine organisms and insects, whereas chitosan rarely occurs in nature and is the result of enzymatic reactions in certain fungi, such as Mucor rouxii [48].

2.5.1 Definition of chitin

Chitin is a high molecular weight biopolymer, non-toxic, and linear, composed of N-acetyl-D-glucosamine units linked by β -D (1- 4) bonds. Chitin is found in the exoskeletons of arthropods such as insects and crustaceans (e.g., crabs and shrimp), as well as in some fungi. It is the second most abundant organic polymer in nature after cellulose.

The earliest research on chitin dates back to 1799, but its discovery is attributed to Henri Braconnot in 1811 when he isolated it from fungi and named it Fungine. Later, in 1823, A. Odier named it Chitin, derived from the Greek word meaning cover or coat. In 1859, C. Rouget discovered its derivative, known as chitosan. The molecular structure of chitin was determined in 1928 by K. H. Meyer and H. Mark [49].

2.5.1.1 Chemical structure

(C8H13O5N)n Chitin consists of a linear polymer whose chain is made up of Nacetyl-2-amino -2- deoxy-D-glucose (GlcNAc) units linked by glycosidic bonds (1- 4), with acetamide groups (CH_3CONH_2) replacing the hydroxyl groups found in cellulose. Chitin is characterized by a crystalline structure thatforms an organized fiber network, imparting mechanical rigidity and strength in living organisms [50]. Chitin is insoluble in water or common organic solvents; however, it dissolves in concentrated acids such as hydrochloric acid and sulfuric acid (at concentrations of 70-97%). When alcohol or acetates are added to these acidic solutions, chitin is re-precipitated in the form of continuous fibers. Its insolubility in water is due to the strong hydrogen bonds between its polymer chains, although it can be chemically converted into soluble derivatives such as chitosan and carboxymethyl chitin [49].

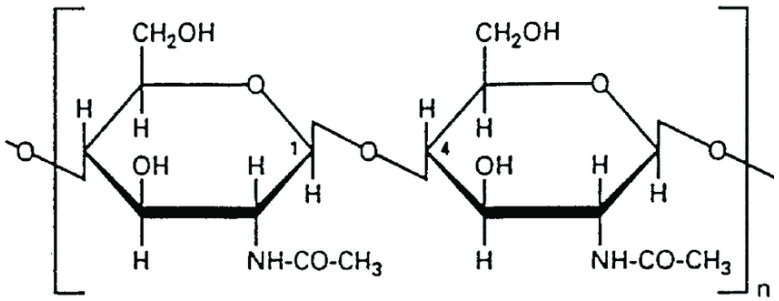

Figure 2.5: Chemical structure of chitin

2.5.2 Definition of chitosan

Chitosan is a polyaminosaccharide and a natural compound from the amino sugar family . It is produced from chitin through a deacetylation reaction using alkaline solutions such as potassium hydroxide. This process involves protein removal and deacetylation[5].

Due to its numerous attractive properties, chitosan contains active amine (-NH2) and hydroxyl (-OH) groups, making it highly effective in removing heavy metals from contaminated water.

The discovery of this compound dates back to the 19th century, when the French scientist Henri Braconnot first extracted chitin from fungal cell walls. Later, in 1859, Roget developed a method to produce chitosan by removing acetyl groups from chitin. Its precise chemical structure was fully identified in the 1950s[51].

2.5.2.1 Chemical composition of chitosan

Chitosan has a chemical structure similar to cellulose, featuring a complex double-helical configuration. It is a linear polysaccharide polymer produced by deacetylating chitin ((1,4)-2-acetamido-2-deoxy--D-glucose). Its molecular weight typically ranges between 50 and 2000 kilodaltons, making it one of the most abundant and sustainable biopolymers in nature. The main structure of chitosan is linked through covalent glycosidic bonds, ensuring significant mechanical strength and chemical stability[52].

The molecular composition of chitosan includes a distinctive set of functional groups, such as:

- A primary hydroxyl group at position C6.
- A secondary hydroxyl group at position C3.
- A free amino group at position C2.

- N-acetyl amino residues and glycosidic bonds.

Among these, the NH2 (amine) and OH (hydroxyl) groups are the most reactive, enabling the formation of various chemical derivatives through reactions such as alkylation or esterification. In contrast, the N-acetyl amino and glycosidic bonds exhibit high chemical stability, requiring stronger reaction conditions or specialized catalysts for modification [53].

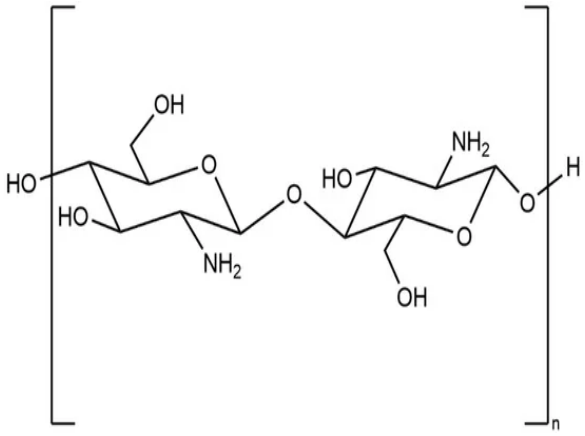

Figure 2.6: Chemical structure of chitosan[2]

2.5.2.2 Properties and Applications of Chitosan

Chitosan possesses unique properties that make it a versatile material across various fields[54]. Some of its key properties include :

- Biocompatibility and biodegradability, making it safe for medical and environmental applications.
- Antibacterial and antiviral properties, enhancing its effectiveness in combating harmful microorganisms.
- Non-toxicity and hypoallergenic nature, allowing its safe use in healthcare and food products.
- High flexibility and elasticity, making it ideal for applications in biofilms and nanofibers.
- Ability to form complex compounds with metal ions and hybrid aromatic carbonates, reinforcing its role in water treatment and pollutant removal.

- Coagulation and flocculation properties, making it valuable in water purification and industrial processes.
- High absorption capacity, efficiently capturing colored substances and organic pollutants, whether in wastewater treatment or air purification.
- Potential for transformation into various derivatives, enabling its use in diverse industries such as medicine, agriculture, and pharmaceuticals [55].

CHAPTER 3

METHODOLOGY

3.1 Introduction

This chapter consists of four sections. The first section describes the properties of the chemicals used in this study. Following by the preparation methods of both the adsorbate and the adsorbent was in section 2. In section 3, the characterization techniques implemented for examining the CHI-HDE/ZnO adsorbent for the removal of Cu^{2+} ions were discussed. These techniques include visible spectroscopy, SEM-EDX, FTIR, and BET surface area analysis. For more details, a schematic representation is designed in Figure 3.3. Finally, the fourth section outlines the controlling variables in Cu^{2+} ions uptake by CHI-HDE/ZnO was simulated by Response Surface Methodology -Box-Behnken Design (RSM-BBD) model, followed by carrying out 29 experiments.

3.2 Chemicals Used and Methods

3.2.1 Chemicals Used

CHI flakes with $\geq$ 75 % degree of deacetylation, and zinc acetate dihydrate (MW: 219.50 g/ mol, MF: $Zn(CH_3COO)_2.2H_2O$) were purchased from Sigma-Aldrich. From Merck: Copper sulfate (MW: 159.61 g/ mol, MF: $CuSO_4$, λ max: 610 nm) was used as an adsorbate. From RM Chemicals: Ammonium hydroxide 30 %, Sulfuric acid 98 %, Ethanoic acid 99.99 %, and caustic soda pellets were supplied. The HDE crosslinker was synthesized following the procedure detailed in our previous study [56]. Throughout this research, Ultra-pure water with a conductivity of 18.2 M cm^{-1} was employed, Table: 3.1 summarizes the physico-chemical properties for some materials and chemical reagents used.

Table 3.1: The key properties for chemicals used.

No	Name	Chemical formula	Properties	Company
1	*CHI*	Polymer	Flakes	Sigma Aldrich
2	*Zinc acetate dihydrate*	$Zn(CH_3COO)_2, 2H_2O$	MW: 219.50 g/mol, solid	Sigma Aldrich
3	*Copper sulfate*	$CuSO_4$	MW: 159.61g/mol. λ: 610 nm. solid	Merck
4	*Ammonium Hydroxide*	NH_4OH	liquid (32%)	RM Chemicals
5	*sulfurie acid*	H_2SO_4	liquid (98%)	RM Chemicals
6	*Ethanoic acid*	CH_3COOH	liquid (99.99%)	RM Chemicals
7	*Sodium Hydroxide*	NaOH	pellets	RM Chemicals

3.2.2 Methods

3.2.2.1 Adsorbate preparation

A stock solution (as presented in Figure 3.1), also called as a mother solution, was prepared by dissolving 1.0 g of copper sulfate powder ($CuSO_4$) in ultra-pure water in a 1 L volumetric flask, resulting in a concentration of 1000 ppm ($1\ g \cdot L^{-1}$). This mother solution was then diluted to obtain the beginning concentrations ranging from 100 to 400 $mg \cdot L^{-1}$, which were consistently used throughout the adsorption experiments [57].

Figure 3.1: Stock Solution of Cu^{2+} ions.

3.2.2.2 Preparation of Zinc Oxide (ZnO)

ZnO powder was prepared from zinc acetate dihydrate via the solution-dropping technique [58]. To conduct this technique, 0.182 g of NaOH was dissolved in a measured volume of ultra-pure deionized water under continuous stirring in a reflux system. Subsequently, zinc acetate dihydrate solution 25 ml (4.56 mmol) was wisely dropped into the solution. The homogeneous mixture (Liquid/Liquid) was heated at 353 K for two hours, resulting in the formation of zinc oxide as a white precipitate. The heterogeneous mixture (solid/liquid) was separated through a filtration technique using a Buchner funnel. The ZnO precipitate was quickly washed and centrifuged at 4000 rpm for 10 minutes until the pH of the supernatant was neutral. The obtained zinc oxide was dried in an oven overnight at 378 K before being converted to a fine powder for the next preparation.

3.2.2.3 Preparation of CHI-HDE/ZnO composite

An optimal ratio of 1 g CHI to 0.25 g ZnO was stirred in aqueous ethanoic acid solution (25 cm^3, 5%). The CHI/ZnO mixture was ultrasonicated for 30 minutes at room temperature to ensure the uniform distribution of zinc oxide into the matrix. The viscous CHI/ZnO combination was transferred as drops into a beaker containing 400 cm^3 of caustic soda solution (0.5 $mol.L^{-1}$), where it changed as a physical modification into beads form. To remove any residual NaOH, the CHI/ZnO beads were repeatedly immersed in ultrapure water, followed by centrifugation at 4000 rpm for 10 minutes. The cross-linking reaction was conducted by converting 10 g of CHI/ZnO beads in a reflux condenser system containing 100 cm^3 of a 2% HDE solution acidified with drops of sulfuric acid, maintained at 353 K for 3 hours. The obtained CHI-HDE/ZnO beads were dried overnight in a hot air oven at 378 K and then ground into a fine powder, resulting in the final polymeric composite, designated as CHI-HDE/ZnO. The prepared CHI-HDE/ZnO composite was characterized using detailed analytical techniques to discover comprehensive insights into its surface properties, effectiveness, and textural characteristics.

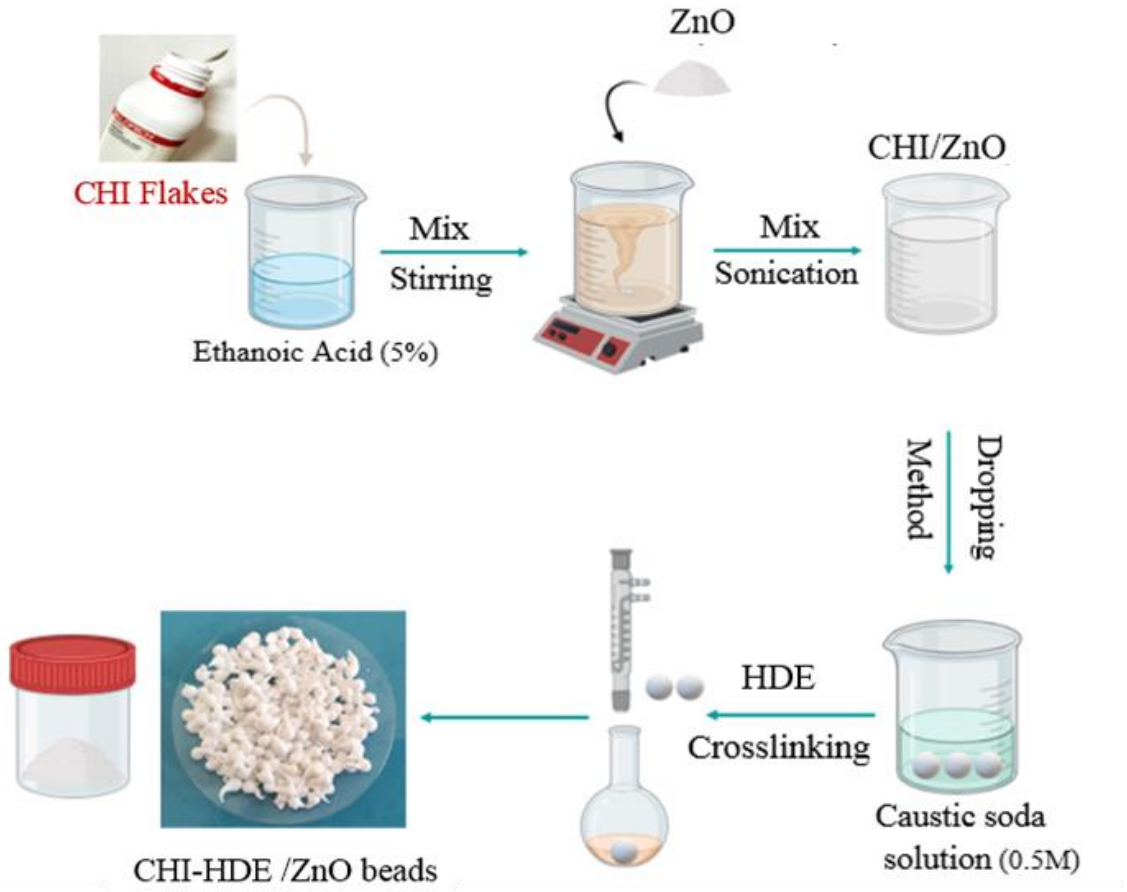

Figure 3.2: Preparation steps for the CHI-HDE/ZnO adsorbent.

3.3 Characterizations

Figure 3.3 represents an overview of the analysis techniques used in this thesis. Surface properties were found out using both Scanning Electron Microscope (SEM)-Energy Dispersive X-Ray (EDX). While the essential functional groups on the CHI-HDE/ZnO surface were detected using Fourier Transform Infrared Spectroscopy (FTIR). To enrich this study in terms of statistics, a statistical mathematical model, RSM-BBD was introduced. The adsorption studies, including thermodynamics, kinetics, and isotherms, were postponed. The instruments and

their respective models used for the analytical techniques mentioned in the introduction (3.1) are detailed below:

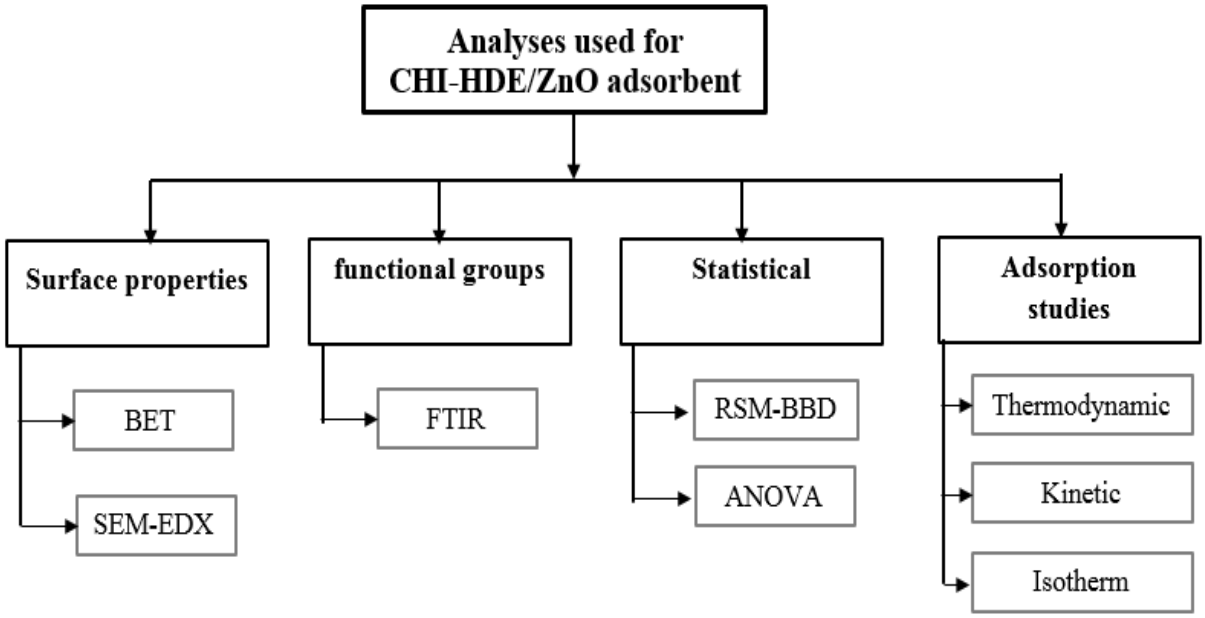

Figure 3.3: Illustrated design of the analyses used for CHI-HDE/ZnO adsorbent.

3.3.1 Visible Spectroscopy Analysis

This device represents an advanced technological solution in the field of chemical and biological analysis, as it is used to analyze precise concentrations of substances in liquids and various compounds. It features a superior optical design based on a dual-beam optical system, ensuring high measurement accuracy and significantly reducing optical interference, in addition to providing stable performance and reliable results with ease of operation. It is also equipped with a high-resolution 6-inch liquid crystal display (LCD) with a resolution of $240 * 320$ pixels, presenting analytical data in an organized and easy-to-read format.

Its engineering design comprises four main units: a radiation source, an advanced lens system, a light sensor, and a digital processing unit. The device operates by analyzing the interaction of light wavelengths with samples, where specific spectra are absorbed according to

the unique chemical properties of each substance. When a dispersed light beam passes through the solution, selective absorption of certain wavelengths occurs based on its chemical composition, leading to a decrease in light intensity. The optical absorption rate is then calculated using mathematical equations that establish a direct relationship between the intensity of absorbed light and the concentration of the target substance, allowing for highly accurate quantification . The Visible device is presented in Figure 3.4

Figure 3.4: Visible instrument

3.3.2 Scanning electron microscopy (SEM-EDX)

It is a type of electron microscope that scans the surface of a sample using a focused electron beam to generate images. The Scanning Electron Microscope (SEM) consists of several main components, including magnetic lenses, a display screen equipped with a computer for data collection and analysis, and an electron source.

The device operates by interacting electrons with the atoms of the sample, generating various signals that provide information about the surface topography and composition of the material. The electron beam is moved in a specific scanning pattern, and the beam's position is correlated with the intensity of the detected signals to form an image. SEM images offer a high level of detail regarding the surface structure of the sample [59].

Figure 3.5: SEM-EDX instrument

3.3.3 Fourier Transform Infrared Spectroscopy (FTIR)

FTIR is an abbreviation for Fourier Transform Infrared Spectroscopy. It is a technique that targets to analyze both inorganic and organic materials by detecting their chemical functional groups and components. The basis of this analysis technique is based on the molecules absorbing energy (infrared rays) generated by the device, which leads to the elongation of bonds or deformation at angles, allowing the determination of their chemical structure. This approach, also known as Fourier Transform Infrared Spectroscopic Analysis, has numerous scientific and industrial applications. In this work, a Fourier Transform Infrared (FTIR) spectroscopy instrument (Model: Shimadzu IR Affnity-1 Japan) was used to identify the functional groups of CHI-HDE-ZnO composite before and after Cu^{2+} adsorption process at absorption bands of 4000 - 400 Cm^{-1}, as shown in Figure 3.7

Overall, an FTIR instrument consists of the following parts:

- Infrared Source
- Sample Compartment
- Wavelength separation
- Detector
- Computer and Fourier Transform Software

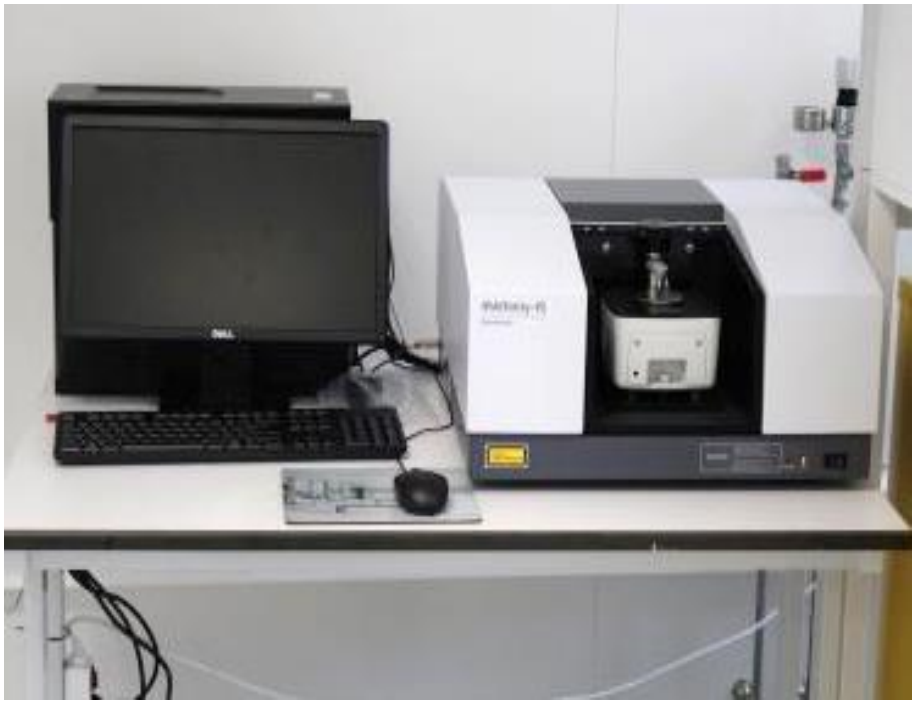

Figure 3.6: FTIR instrument

3.3.4 BrunauerEmmett Teller (BET)

Measuring surface properties is a crucial aspect of studying a wide range of materials, making the BET device an essential tool used by researchers and engineers to analyze material surfaces and evaluate their physical and chemical properties.

This device consists of three main components :

- The main unit, which includes the furnace, vacuum pump, electrical circuit, and electronic measuring device.
- Drainage cells.
- Control system.

The device operates based on the adsorption of nitrogen gas onto the surface of the sample being measured. When activated, the gas flows into the analysis cell, and excess molecules are removed until an extremely low pressure is achieved within the cell. Due to nitrogens high affinity for solid surfaces with fine pores, it quickly adheres to the samples surface.

Subsequently, electronic signals are analyzed to determine the amount of adsorbed nitrogen, enabling the calculation of the actual surface area of the sample. Repeating this process

enhances the accuracy of measurements by removing excess molecules and re-measuring adsorption, providing precise data on the materials porosity and surface area.

Figure 3.7: BET instrument

3.4 Design of trials based on BBD-RSM

The Design Expert 13.0, Stat-Ease, was executed as an excellent tool for trials modeling and minimizing additional effort and operating costs [60]. In this current work: four controlling variables, namely, CHI-HDE/ZnO , pH , adsorption time, and temperature, were input using box-behnken design (BBD) in response surface methodology (BBD-RSM) approach to assess the potency adsorption capacity of Cu^{2+} ions by CHI-HDE/ZnO adsorbent under diverse environmental variables. Table 3.2 presents the terms, controlling variables, and their respective levels for Cu^{2+} ions in the BBD. It is worth noting that the levels of the controlling variables were determined based on preliminary tests. A total of 29 trials, resulting in 5 center point runs for error calculation, were performed to evaluate the effectiveness of CHI-HDE/Zn in removing Cu^{2+} ions. The relationship between the variables and the response was determined using a second-order polynomial model, as expressed in the following equation 3.1.

$$Y = \beta_0 + \sum_{j=1}^{m} \beta_j x_j + \sum_{j=1}^{m} \beta_{jj} x_j^2 + \sum \sum_{i<j=2}^{m} \beta_{ij} x_i x_j \tag{3.1}$$

In this context, Y represents the predicted response (percentage removal of Cu^{2+}), β_0 denotes the constant term, β_j indicates the linear effect of the input variable, β_{jj} corresponds to the quadratic coefficient of the input variable, and β_{ij} represents the interaction coefficient between the input variables x_i and x_j.

Table 3.2: Terms, Controlling variables, and their levels in the BBD for Cu^{2+}

		Levels		
Term	**Controlling variables**	**Lowest (-1)**	**Centre (0)**	**Highest (+1)**
A	CHI-HDE/ZnO (g)	0.04	0.07	0.1
B	pH	3	4.3	5.6
C	adsorption time (min)	10	20	30
D	Temperature (Kelvin)	303	313	323

Table 3.3: The 4- variables BBD matrix and experimental data of adsorption capacity (q_e)for Cu^{2+} .

Run	**A**: CHI-HDE/ZnO	**B**: pH	**C**: adsorption time	**D**: Temperature	Cu^{2+} $(\mathbf{mg \cdot g^{-1}})$
1	0.04	3	20	313	117.8
2	0.1	3	20	313	57.14
3	0.04	5.6	20	313	146.4
4	0.1	5.6	20	313	**9**4.28
5	0.07	4.3	10	303	89.79
6	0.07	4.3	30	303	100.1
7	0.07	4.3	10	323	97.95
8	0.07	4.3	30	323	112.2
9	0.04	4.3	20	303	139.2
10	0.1	4.3	20	303	80. 01
11	0.04	4.3	20	323	160.7
12	0.1	4.3	20	323	87.14

13	0.07	3	10	313	69.38
14	0.07	5.6	10	313	97.95
15	0.07	3	30	313	75.51
16	0.07	5.6	30	313	112.2
17	0.04	4.3	10	313	153.5
18	0.1	4.3	10	313	71.42
19	0.04	4.3	30	313	139.2
20	0.1	4.3	30	313	91.42
21	0.07	3	20	303	71.42
22	0.07	5.6	20	303	102.0
23	0.07	3	20	323	79.59
24	0.07	5.6	20	323	114.2
25	0.07	4.3	20	313	102.1
26	0.07	4.3	20	313	102.1
27	0.07	4.3	20	313	97.95
28	0.07	4.3	20	313	97.95
29	0.07	4.3	20	313	100.1

In batch adsorption tests, the experiments were carried out using 100 cm^3 of Cu^{2+} adsorbate solutions (100 mg/L) with pH values ranging from 3 to 5.6. The adsorbent dose was varied between 0.04 and 0.1 g, while the equilibration adsorption time was adjusted from 10 to 30 minutes. The temperature was set within the range of 303 to 323 K, as summarized in Table 3.3. Following adsorption, the absorbance (A) corresponding to each run was measured using a UV-visible spectrophotometer (Model: UviLine 9600 UVVISIBLE, SECOMAN, France) at a wavelength of 610 nm for Cu^{2+} after complexing with a 30% ammonia hydroxide solution. The calibration curve of Cu^{2+} ions (as plotted in Fig. 3.8) and equation 3.2 the were used to determine the initial and equilibrium concentrations, while the amount of Cu^{2+} ions adsorbed

was calculated using equation 3.3.

$$A = \varepsilon \, l \, C \tag{3.2}$$

$$q_e = V \frac{C_0 - C_e}{W} \tag{3.3}$$

where ε denotes the molar absorptivity ($\mathrm{L \cdot mol^{-1} \cdot cm^{-1}}$), L denotes the path length of the cuvette (cm), V represents the volume of the Cu^{2+} adsorbate solution ($\mathrm{cm^3}$), and W refers to the weight of the adsorbent used (g).

As evident from Run 11 (Table 3.3), the highest adsorption capacity of Cu^{2+} from the aqueous solution was attained to be 160.7 mg/g, achieved under multivariable conditions: 0.04 g of CHI-HDE/ZnO, pH around 4.3, an adsorption time of 20 minutes, and a temperature of 323 K. This set of experimental conditions was therefore established as the optimal parameters for subsequent adsorption studies.

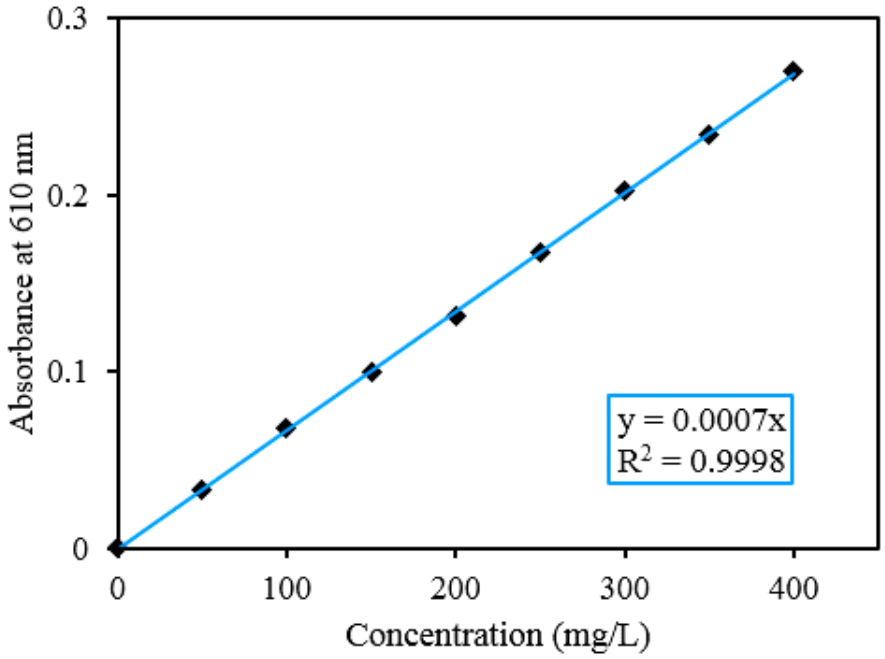

Figure 3.8: Calibration Curve of Cu^{2+} ions: Absorbance vs. Concentration.

At the end of this chapter, it's worth noting that analytical techniques are among the fundamental pillars researchers rely on to prove the accuracy and validity of their findings. Although there are many analytical techniques that we were unable to use in this study due to limited resources, we were keen to employ the most prominent and effective ones to achieve the research objectives.

CHAPTER 4

RESULTS AND DISCUSSION

In the concluding chapter, It focuses on the analysis and discussion of the results of the CHI-HDE/ZnO adsorbent prepared from the biopolymer chitosan. This material has proven its efficiency in adsorbing divalent ions from aqueous media, even in acidic media. Through an in-depth study, this chapter aims to shed light on the performance of this innovative material and its potential applications.

4.1 Results And Discussion

4.1.1 Characterization

4.1.1.1 SEM-EDX Analysis

The morphology of CHI, CHI-HDE/ZnO, and CHI-HDE/ZnO after Cu^{2+} adsorption was characterized using SEM images at a magnification of 1300x, as shown in Fig.4.1 (a, c, and e). For CHI, visible cavities with protrusions randomly distributed were observed on its smooth surface. Additionally, carbon, oxygen, and nitrogen were detected as fundamental elements in the chitosan backbone (refer Fig.4.1,a-b). A noticeable change in the morphology of the chitosan surface after loading ZnO on it can be observed, as it was rougher and more wrinkled and the smooth surface had vanished (Fig.4.1,c). The wrinkled and rough topography contributed to the retention of heavy metal ions of Cu^{2+} on the CHI-HDE/ZnO's surface. The distributed elements of carbon, oxygen, nitrogen, zinc, copper, and sulfur on the surface were further verified by Energy Dispersive X-ray Spectroscopy (Fig.4.1,d,f), indicating the successful adsorption process.

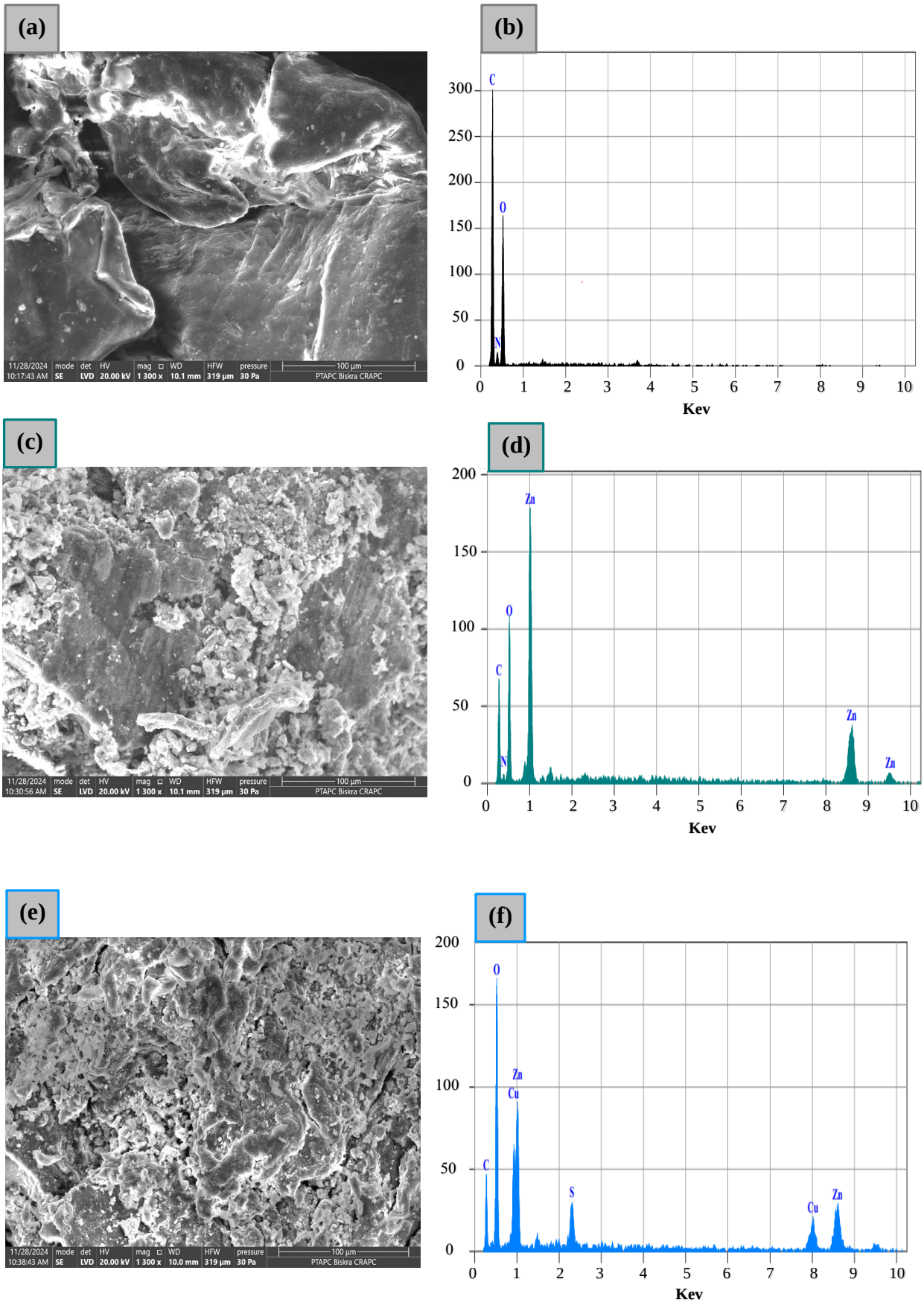

Figure 4.1: SEM and EDX spectra: (a,b) CHI,(c,d) CHI-HDE/ZnO, and (e,f) CHI-HDE/ZnO after adsorption of Cu^{2+} ions

4.1.1.2 FT-IR spectral results

The significant structural functions of bio-based adsorbent were characterized utilizing infrared spectroscopy. FTIR spectra of CHI-HDE/ZnO, Cu^{2+} ions adsorbed by CHI-HDE/ZnO, and the comparison between them are displayed in Fig.4.2 (a,b, and a+b). The broad band at 3395.1 cm^{-1} is attributed to the stretching vibration of -OH ascribing to alcohol functional groups [61], while the low-intensity peak at 2818.8 cm^{-1} corresponds to the C-H symmetric/asymmetric bending vibration of alkyl group in the CHI-HDE/ZnO structure. The presence of an aromatic ring was reaffirmed by weak intensity peaks at 1577.6 cm^{-1} and 3096.9 cm^{-1}, corresponding to the C=C and C-H aromatic vibrations, respectively. Similarly, ZnO and CHI crosslinking are identified by the distinct bands observed at 1672.3 cm^{-1} and 423.7 cm^{-1}, respectively. It is evident that certain absorption bands became broader compared to those prior to Cu^{2+} removal, accompanied by slight shifts. Notably, the absorption peak of the hydroxyl group shifted from 3395.1 cm^{-1} to 3401.4 cm^{-1}, while the absorption peak of the imine group shifted from 1672.0 cm^{-1} to 1661.0 cm^{-1} (refer to IR spectrum a+b), indicating that surface functional groups, such as hydroxyl, Schiff's base, and hydrogen bonding, significantly influenced the performance of the Cu^{2+} adsorption process.

Table 4.1: The distinct shifts in wavenumbers for Cu^{2+} adsorption by CHI-HDE/ZnO composite.

Function / Group	**Wavenumber (cm^{-1})**	**Shift to**
O-H	3395.1	3401.4
C-H	2818.8	2806.2
C=N	1672.3	1660.7
C-O	1074.7	1092.7

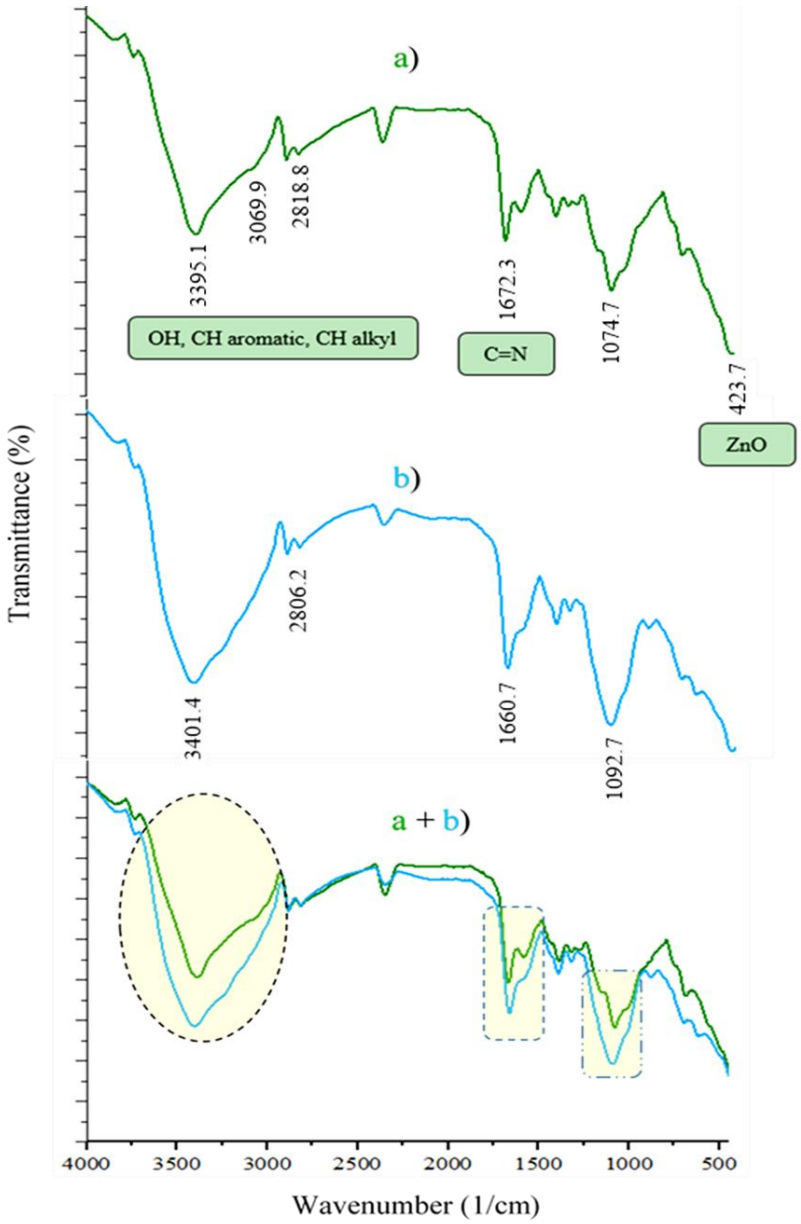

Figure 4.2: FTIR spectra of : a) CHI-HDE/ZnO, and b) CHI-HDE/ZnO + Cu^{2+} ions.

4.1.1.3 Surface properties

The surface area plays a pivotal role in the adsorption process, which directly reflects on the efficiency of the adsorbent. Typically, a larger surface area corresponds to greater adsorption capacity and enhanced removal efficiency [62]. Table 4.2 presents the surface areas of CHI, $CHI-HDE$, and CHI-HDE/ZnO. According to the data, CHI has a BET surface area of 0.401 m^2/g, while $CHI-HDE$ exhibits a higher value of 0.666 m^2/g. The most significant increase is observed in CHI-HDE/ZnO, which reaches 3.762 m^2/g. These results indicate that the Schiff base crosslinking between chitosan and synthesized CHI effectively enhanced the surface area, increasing it by 1.66 times. Additionally, the uniform incorporation and dispersion of ZnO particles within the $CHI-HDE$ polymer matrix further elevated the surface area by 5.64 times. The graphical pore distribution characteristics of CHI-HDE/ZnO are plotted in Fig. 4.3. It can be observed from Fig 4.3 that the adsorption and desorption curves exhibit a narrow hysteresis loop, remaining horizontally parallel between 0.1 and 0.85 before transitioning into a vertical shape at higher relative pressures. This behavior suggests that the CHI-HDE/ZnO adsorbent possesses a mesoporous structure type IV with an H1 isotherm, as classified by IUPAC [63]. This thus leads to the conclusion that chitosan modification not only improved the surface area (from 0.401 to 3.762 m^2/g) but also reinforced its chemical and mechanical stability under acidic conditions, as evidenced by its high adsorption efficiency for Cu^{2+} ions, achieving 90.43% at pH 5.6 (Table 3.3, run 4).

Table 4.2: Surface properties of CHI, $CHI-HDE$, and CHI-HDE/ZnO.

Parameter(s)	**CHI**	$CHI-HDE$	**CHI-HDE/ZnO**
BET Surface Area (m^2/g)	0.401	0.666	3.762
Langmuir Surface Area (m^2/g)	0.522	0.869	9.221
Average Particle Size (nm)	14944	9000.9	1594.9

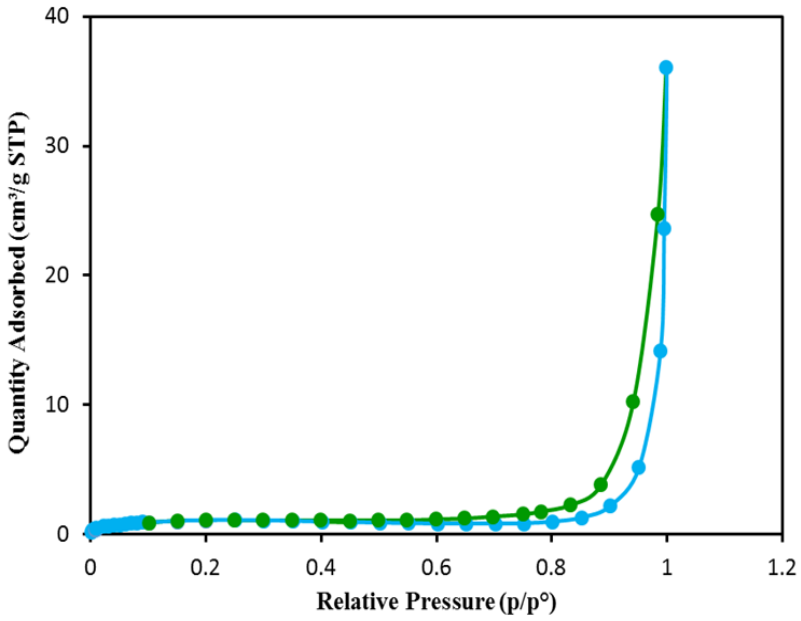

Figure 4.3: Nitrogen adsorption-desorption isotherms of CHI-HDE/ZnO at 77k.

4.1.2 Statistical analysis

Analysis of variance (ANOVA) is a statistical method used to validate experimental BBD results by finding a strong agreement between the experimental and statistically expected values [64]. Table 4.3 exhibits the ANOVA outcomes for the adsorption capacity of Cu^{2+} ions. From Table 4.3, the F-value of 133.57 implies that the experimental data from BBD are amenable to statistical analysis. This observation can be supported by the high values of the correlation coefficients (R^2 =0.9926, adjusted R^2 =0.9851), indicating a strong model fit between the predicted and actual values for Cu^{2+} adsorption capacity. Additionally, the adequate precision value of 45.2206, substantially exceeding the recommended threshold of 4, further confirms the model's reliability [65; 66]. According to the conditions of model, all four terms listed in Table 3.2 (A, B, C, and D) are significant [67], contributing to raise the adsorption capacity from 57.15 to 160.7 mg/g (refer to Table 3.3). Hence, from the above interpretation, the relationship between the controlling variables and Cu^{2+} adsorption capacity results (response) was established using a second-order polynomial model, formulated after excluding non-significant terms ($p > 0.05$), as presented in Equation 4.1a.

$$\begin{aligned} Cu^{2+}\text{ adsorption capacity } (\text{mg}\cdot\text{g}^{-1}) = {} & +100 - 31.30\text{A} + 16.36\text{B} + 4.21\text{C} \\ & + 5.78\text{D} + 8.57\text{AC} \\ & - 3.57\text{AD} + 14.77\text{A}^2 - 10.27\text{B}^2 \end{aligned} \tag{4.1a}$$

Table 4.3: Analysis of variance (ANOVA) of the adsorption capacity (q_e) for Cu^{2+}

q_e (Cu^{2+}, $mg.g^{-1}$)					
Source	**Sum of Squares**	**Df**	**Mean Square**	**F-value**	**p-value**
Model	18581.25	14	1327.23	133.57	< 0.0001
A: (CHI-HDE/ZnO)	11763.44	1	11763.44	1183.88	< 0.0001
B: (pH)	3212.01	1	3212.01	323.26	< 0.0001
C: (Adsorption time)	213.47	1	213.47	21.48	0.0004
D: (Temperature)	401.22	1	401.22	40.38	< 0.0001
AB	18.37	1	18.37	1.85	0.1955
AC	293.88	1	293.88	29.58	< 0.0001
AD	51.02	1	51.02	5.13	0.0398
BC	16.66	1	16.66	1.68	0.2163
BD	4.16	1	4.16	0.42	0.5278
CD	4.16	1	4.16	0.42	0.5278
A^2	1416.75	1	1416.75	142.58	< 0.0001
B^2	684.43	1	684.43	68.88	< 0.0001
C^2	9.19	1	9.19	0.93	0.3524
D^2	20.29	1	20.29	2.04	0.1749
Residual	139.11	14	9.94		
Lack of Fit	122.45	10	12.24	2.94	0.1551
Pure Error	16.66	4	4.16		
Cor Total	18720.35	28			

$R^2 = 0.9926$, $R^2_{\text{adj}} = 0.9851$, Adequate Precision = 45.2206

The interactions between the controlled variables that impact Cu^{2+} adsorption offer further proof of the reliability of the empirical BBD results. Based on Equation 4.1a, two types of binary statistical interactions were identified and visualized through 3D surface and 2D contour plots, shown in Figure 4.4. AC represents binary statistical interaction between CHI-HDE/ZnO and pH effect on Cu^{2+} adsorption with a p-value less than 0.0001, while controlled variables are maintained constant: adsorption time (20 minutes) and temperature (323 K). The corresponding 3D response surface and 2D contour plots illustrating this interaction are

presented in Figures 4.4a and 4.4b, respectively. It can be vividly seen from Figures 4.4a and 4.4b that the remarkable increase in Cu^{2+} adsorption capacity value from 51.14 to 160.7 mg/g under an acidic medium resulted from an increase in CHI-HDE/ZnO from 0.04 to 0.1 g. This finding is ascribed to the increased probability of Cu^{2+} ions binding to the available active adsorption sites of CHI-HDE/ZnO, resulting from increased surface area.

Another binary statistical interaction (p = 0.0398) was observed between CHI-HDE/ZnO and temperature (denoted as interaction AD), while the Cu^{2+} adsorption time was set at 20 min in the acidic environment of the solution. Figures 4.4c and 4.4d, which represent the 3D surface and 2D contour plots of AD interaction, respectively, reveal that Cu^{2+} adsorption capacity is influenced by raising the temperature from 303 to 323 K. This observation likely predicts that the adsorption process of Cu^{2+} ions by CHI-HDE/ZnO will be endothermic in nature.

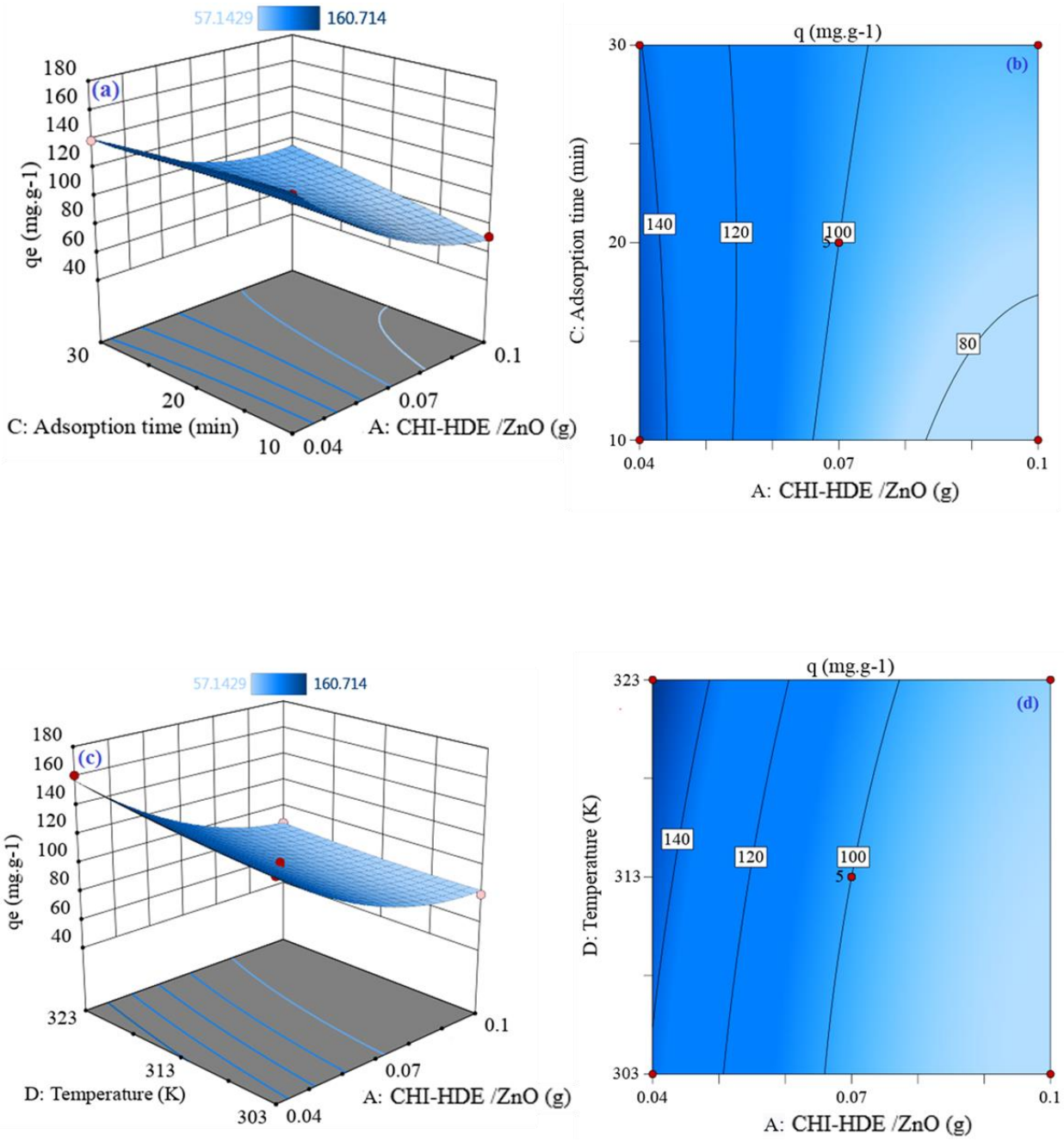

Figure 4.4: Binary statistical interaction of adsorption capacity for Cu^{2+} ions: a-c) 3D response surface, b-d) 2D contour plot.

4.1.3 Adsorption study

To evaluate the efficiency of CHI-HDE/ZnO as a promising adsorbent for capturing Cu^{2+} ions from an aqueous medium, the concentration gradient test was adopted [68]. In this regard, six different beginning concentrations ranging from 100 to 400 mg $\cdot$ L^{-1} were used in this batch adsorption study, with other independent variables, including the CHI-HDE/ZnO dose = 0.04 g, pH = 4.3, and temperature = 323 K, held constant. Fig.4.5 elucidates the adsorption capacity (mg $\cdot$ g^{-1}) of Cu^{2+} ions onto CHI-HDE/ZnO as a function of adsorption time (min). It is evident from Fig. 4.5 that increasing the concentration gradient of Cu^{2+} ions from 100 to 400 mg/L requires extra absorption time, with adsorption equilibrium platform being reached at 30 minutes for concentrations of 100 and 150 mg/L, 40 minutes for 200 mg/L, and 60 minutes for 250, 300, and 400 mg/L. This is likely interpreted by the crowded movement caused by an increase in the number of Cu^{2+} ions toward the active adsorption sites within the CHI-HDE/ZnO surface [69]. Hence, the acceptable value of adsorption capacity, which was found to be 280 mg/g at high concentration in a short time, may reflect the ability of CHI-HDE/ZnO to capture other types of heavy metal ions from aqueous mediums.

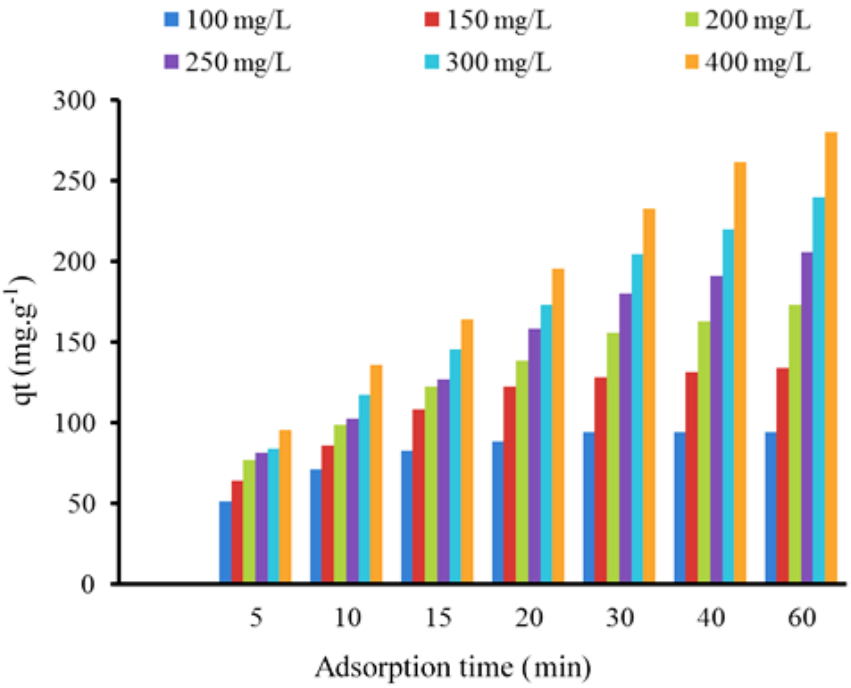

Figure 4.5: Adsorption efficiency of Cu^{2+} ions onto CHI-HDE/ZnO at different initial concentrations as a function of adsorption time (does = 0.04 g, pH= 4.3, Temp = 323K, Cu^{2+} ions Vol =100 cm^3).

4.1.3.1 Thermodynamic study

It is extremely important to provide evidence that the adsorption process has occurred. For this reason, a thermodynamic study has been carried out [70]. Three thermodynamic state functions were applied to obtain the adsorption thermodynamic results of Cu^{2+} adsorption by CHI-HDE/ZnO. For more details, the change for Gibbs free energy (ΔG, kJ $\cdot$ mol^{-1}) was calculated using equation 4.2, whereas the change in entropy (ΔS, J $\cdot$mol$^{-1}\cdot$K^{-1}) and enthalpy (ΔH, kJ$\cdot$mol^{-1}) were inferred from the plot of Gibbs free energy versus temperature, presented in Fig. 4.6 [71]. The thermodynamic output data (detailed in Table 4.4) reveal that the amount of adsorbed Cu^{2+} ions increased with increasing in K_d from 4.46 to 9.14 L$\cdot$g^{-1}. Additionally, the adsorption process of Cu^{2+} by CHI-HDE/ZnO was spontaneous at all working temperatures. This observation is likely to concur with the negative values of ΔG ranging from -3.76 to -6.12 kJ $\cdot$ mol^{-1}. Furthermore, the significantly positive ΔS value (76.7 J $\cdot$ mol^{-1} $\cdot$ K^{-1}) suggests an increase in randomness, facilitating the binding of Cu^{2+} ions to the CHI-HDE/ZnO surface. As a result, the ΔG and ΔS values provided strong evidence for the occurrence of Cu^{2+} ions adsorption by CHI-HDE/ZnO, accompanied by an endothermic enthalpy change (ΔH = 19.0 kJ $\cdot$ mol^{-1}) during this process.

$$\Delta G = -RT \ln K_d \tag{4.2}$$

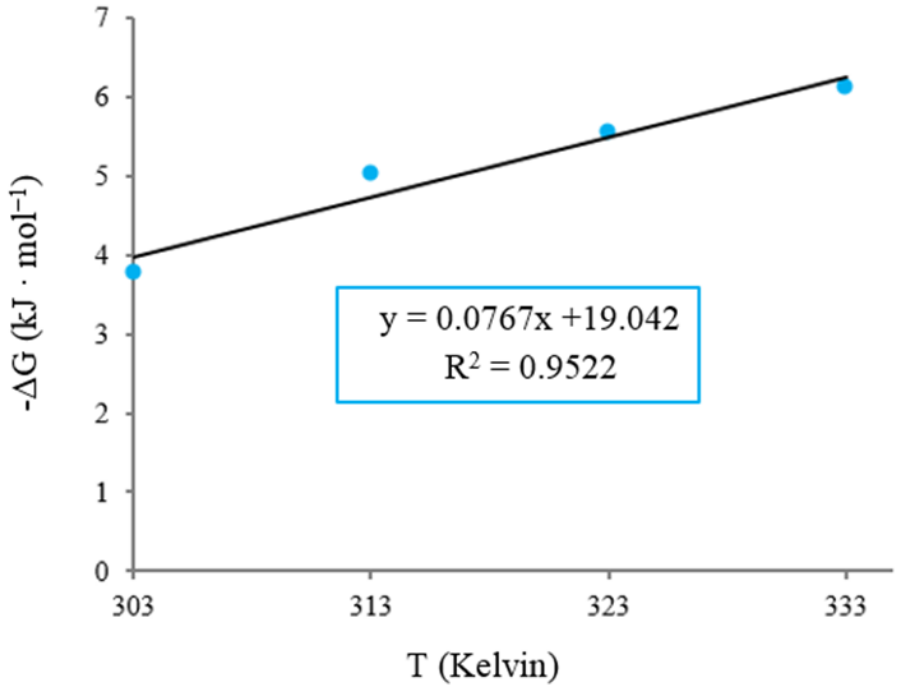

Figure 4.6: Gibbs free energy (G) versus temperature plot for Cu^{2+} ions adsorption by CHI-HDE/ZnO (dose = 0.04 g, pH = 4.3, solution concentration = 100 ppm, and vol. = 100 mL).

Table 4.4: The adsorption thermodynamic results for Cu^{2+} adsorption by CHI-HDE/ZnO.

T (Kelvin)	K_d $(\mathbf{L \cdot g^{-1}})$	ΔH $(\mathbf{kJ \cdot mol^{-1}})$	ΔS $(\mathbf{J \cdot mol^{-1} \cdot K^{-1}})$	ΔG $(\mathbf{kJ \cdot mol^{-1}})$
303	4.46			**-3.76**
313	6.89	19.0	76.7	**-5.02**
323	7.87			**-5.54**
333	9.14			**-6.12**

4.1.3.2 Adsorption Kinetics

Adsorption kinetic results are always of great significance in determining the nature of the adsorption process, whether it involves physisorption or chemisorption [72]. For this purpose, the experimental kinetic data of Cu^{2+} ions adsorption on CHI-HDE/ZnO were simulated using two kinetic models, namely the pseudo-first-order (PFO) and the pseudo-second-order (PSO) [73; 74], and are expressed as seen in non-linear equations 4.3 and 4.4 .

$$q_t = q_e \left(1 - \exp(-K_1 t)\right) \tag{4.3}$$

$$q_t = \frac{t}{(\frac{1}{K_2 q_e^2}) + (\frac{t}{q_e})} \tag{4.4}$$

Herein, qt and qe denote the amount of Cu^{2+} ions adsorbed at time t (in minutes) and at equilibrium, respectively. The velocity constant of the PFO and PSO are represented by K_1 and K_2, respectively.

Table 4.5 illustrates results simulated by fitting PFO, and PSO kinetic models for Cu^{2+} sorption by CHI-HDE/ZnO. A high correlation coefficient (R^2), a high-velocity constant (k), and a low Root Mean Square Error (RMSE) are supported to determine the best-fitting kinetic model for the experimentally simulated data [75]. Based on these criteria, It can be clearly confirmed that the sorption kinetics of Cu^{2+} ions on CHI-HDE/ZnO was well fitted by a pseudo-second-order model, indicating that the strong bonds played a leading role in the chemisorption process of Cu^{2+} ions by CHI-HDE/ZnO [76].

Table 4.5: results simulated by fitting PFO, and PSO kinetic models for Cu^{2+} sorption by CHI-HDE/ZnO.

Kinetic model	Parameter	Cu^{2+} $C_o(m\mathbf{mg}\cdot\mathbf{L}^{-1})$						Average
		100	150	200	250	300	400	
Pseudo-first order (PFO)	$q_{\exp}$ $(\mathbf{mg}\cdot\mathbf{g}^{-1})$	94.29	134.2	172.8	205.7	240.1	280.1	
	$q_{e\mathbf{cal}}$ $(\mathbf{mg}\cdot\mathbf{g}^{-1})$	94.20	133.3	167.5	203.5	238.4	281.4	
	k_1**(1/min)**	0.148	0.115	0.094	0.074	0.067	0.063	
	R^2	0.993	0.991	0.987	0.985	0.992	0.991	
	$RMSE$	1.281	3.557	6.853	8.835	7.662	9.726	**6.319**
Pseudo-second order (PSO)	$q_{e\mathbf{cal}}$ $(\mathbf{mg}\cdot\mathbf{g}^{-1})$	106.3	155.1	199.2	251.1	299.6	357.1	
	$k_2\times10^{-2}$**(g/mg min)**	0.196	0.093	0.055	0.031	0.022	0.017	
	R^2	0.998	0.994	0.996	0.991	0.997	0.996	
	$RMSE$	2.771	4.652	3.781	6.941	4.621	6.328	**4.849**

4.1.3.3 Adsorption isotherm

The adsorption isotherm was studied to estimate the maximum adsorption capacity of Cu^{2+} adsorbed by CHI-HDE/ZnO at a constant temperature and to describe the nature of the adsorbent surface, whether homogeneous or heterogeneous. To achieve this, the experimental isotherm data was analyzed using three non-linear isotherm formulas corresponding to the most widely used isotherm models: Langmuir [77], Freundlich [78], and Temkin [79]. The isotherm models and their corresponding parameters for Cu^{2+} adsorption by CHI-HDE/ZnO are listed in Table 4.6, while the respective curve representations are plotted in Fig. 4.7. To determine the best model for the experimental isotherm data, the regression coefficient values (R^2) and Root Mean Square Errors (RMSE) were taken into account. Accordingly, Langmuir was the best fit for the experimental isotherm data, as depicted by the high R^2 and low RMSE values tabulated in Table 4.6. In addition, the maximum adsorption capacity was measured to be 327.8 $\mathrm{mg}\cdot\mathrm{g}^{-1}$. These outcomes indicate that ZnO played a pivotal role in coating the cavities on the CHI surface, as illustrated in Fig. 4.1 a, resulting in the formation of a uniform and homogeneous surface. Furthermore, CHI-HDE/ZnO exhibited the ability to interact with Cu^{2+} ions, facilitating the formation of a monolayer during the chemisorption process.

The adsorption capacity of Cu^{2+} by CHI-HDE/ZnO was compared with that of various adsorbents previously reported for Cu^{2+} adsorption, as listed in Table 4.7. Based on the mentioned literature in Table 4.7, the higher adsorption capacity was achieved using a small amount of CHI-HDE/ZnO of 0.04g within a short adsorption time of 20 min for a high concentration of 400 $mg \cdot L^{-1}$. Hence, CHI-HDE/ZnO may be condidated as a promising adsorbent for other possible significant applications.

Table 4.6: Isotherm models and their corresponding parameters for Cu^{2+} adsorption by CHI-HDE/ZnO.

Model	**formulas**	**Parameters**	**value**
Langmuir	$q_e = \frac{C_e}{\frac{1}{q_{max}K_L}+\frac{C_e}{q_{max}}}$	q_{max} $(mg \cdot g^{-1})$	327.8
		$K_L(L \cdot mg^{-1})$	0.05
		$RMSE$	6.25
		R^2	0.99
Freundlich	$q_e = K_f C_e^{1/n}$	n	2.65
		K_f $(L \cdot g^{-1})$	51.40
		$RMSE$	13.1
		R^2	0.96
Temkin	$q_e = \frac{RT}{b_T}\ln(K_T C_e)$	b_T $(J \cdot mol^{-1})$	34.19
		K_T $(L \cdot g^{-1})$	0.48
		$RMSE$	8.19
		R^2	0.98

Table 4.7: Adsorption capacity of Cu^{2+} ions by different adsorbents.

Adsorbents	**adsorption capacity** $(\mathbf{mg \cdot g^{-1}})$	**References**
Chitosan	**16.80**	[80]
Chitosan Beads	**64.62**	[81]
Activated Carbon/Chitosan	**71.99**	[82]
Chitosan Schiff's base (CSTG)	**76.1**	[83]
Clay Chitosan	**94.14**	[84]
Carboxymethylated Cellulose Chitosan (CMCC)	**169.5**	[85]
Magnetic Chitosan	**216.6**	[62]
ASB-MGM	**248.1**	[86]
Commercial ZnO powders	**315.6**	[87]
CHI-HDE/ZnO	**327.8**	This work

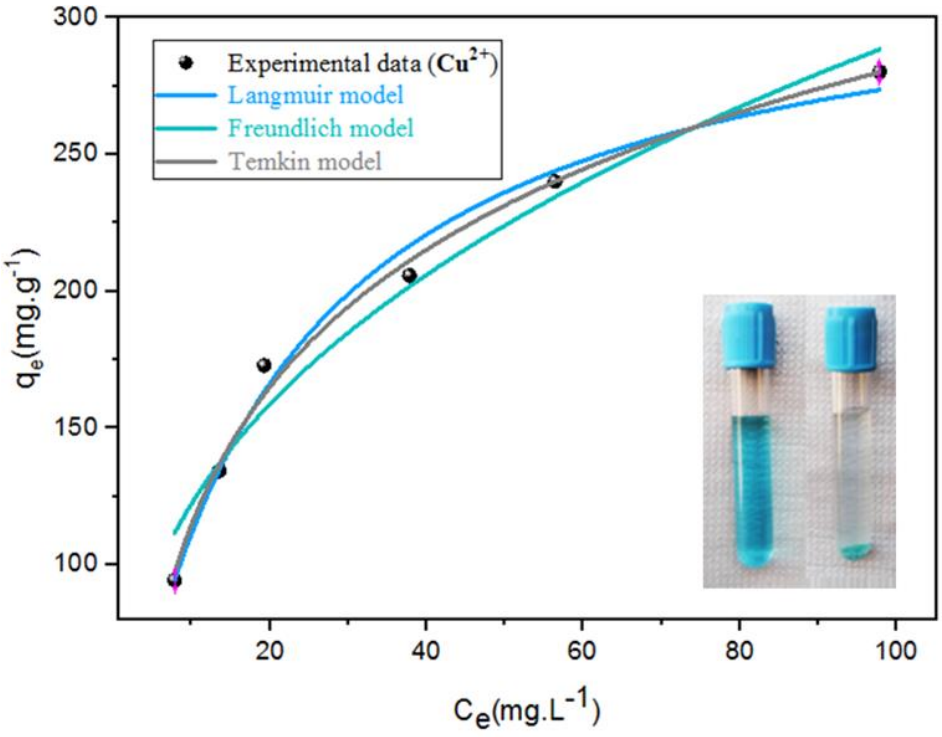

Figure 4.7: adsorption isotherms of Cu^{2+} removal by CHI-HDE/ZnO

CONCLUSION

In conclusion, this study contributes to the introduction of Schiff-based chitosan (CHI-HDE/ZnO) as an excellent adsorbent for the efficient removal of Cu^{2+} ions from water systems. CHI-HDE/ZnO was successfully synthesized by loading with zinc oxide, followed by crosslinking with 2-Hydroxy-1,2-Di(phenyl)Ethanone. Several analyses, including surface properties (BET, SEM-EDX), functional groups (FTIR), statistical (ANOVA), and adsorption studies (Thermodynamic, Kinetic, and isotherm models), were employed to assess of efficiency of Cu^{2+} removal by CHI-HDE/ZnO adsorbent. A batch adsorption approach was implemented using Box-Behnken design (BBD) to evaluate the performance of CHI-HDE/ZnO amids multivariable environments, where the highest adsorption capacity of Cu^{2+} by CHI-HDE/ZnO reached of 160.7 mg/g at the optimum condition: beginning concentration = 100 mg/L, CHI-HDE/ZnO = 0.04 g, pH around 4.3, an adsorption time = 20 minutes, and a temperature = 323 K. Under these conditions, the analysis of variance (ANOVA) statistical method detected two significant binary interaction variables: AC (P-value $<$ 0.0001) and AD(P-value = 0.0398). The thermodynamic study introduced conclusive evidence that the adsorption process is feasible and spontaneous, as indicated by the negative ΔG values at all working temperatures. Additionally, the positive ΔS value suggests increased randomness, reaffirming the favorable passage of Cu^{2+} ions towards the CHI-HDE/ZnO surface. The pseudo-second-order model precisely describes the experimental kinetic data, reaching the adsorption equilibrium within 60 min at a beginning concentration of 400 mg/L. The maximum adsorption capacity qmax (327.8 mg/g) was measured at 0.04 g of CHI-HDE/ZnO, based on the Langmuir isotherm model. As a above findings, CHI-HDE/ZnO could be candidated as an excellent adsorbent for the elimination of heavy metals, including Copper (II), from wastewater.

BIBLIOGRAPHY

[1] R. Singh, N. Gautam, A. Mishra, and R. Gupta, "Heavy metals and living systems: An overview," *Indian journal of pharmacology*, vol. 43, no. 3, pp. 246–253, 2011.

[2] D. Yan, Y. Li, Y. Liu, N. Li, X. Zhang, and C. Yan, "Antimicrobial properties of chitosan and chitosan derivatives in the treatment of enteric infections," *Molecules*, vol. 26, no. 23, p. 7136, 2021.

[3] D. Banerjee, "Water pollution and human health," 2017.

[4] K. H. H. Aziz, F. S. Mustafa, K. M. Omer, S. Hama, R. F. Hamarawf, and K. O. Rahman, "Heavy metal pollution in the aquatic environment: efficient and low-cost removal approaches to eliminate their toxicity: a review," *RSC advances*, vol. 13, no. 26, pp. 17 595–17 610, 2023.

[5] M. Ahmad, S. Ahmed, B. L. Swami, and S. Ikram, "Adsorption of heavy metal ions: role of chitosan and cellulose for water treatment," *Langmuir*, vol. 79, pp. 109–155, 2015.

[6] K. H. H. Aziz, F. S. Mustafa, R. F. Hamarawf, and K. M. Omer, "Adsorptive removal of toxic heavy metals from aquatic environment by metal organic framework (mof): A review," *Journal of Water Process Engineering*, vol. 70, p. 106867, 2025.

[7] L. Zhang, Y. Zeng, and Z. Cheng, "Removal of heavy metal ions using chitosan and modified chitosan: A review," *Journal of Molecular Liquids*, vol. 214, pp. 175–191, 2016.

[8] I. Aranaz, A. R. Alcántara, M. C. Civera, C. Arias, B. Elorza, A. Heras Caballero, and N. Acosta, "Chitosan: An overview of its properties and applications," *Polymers*, vol. 13, no. 19, p. 3256, 2021.

[9] S. G. Kou, L. M. Peters, and M. R. Mucalo, "Chitosan: A review of sources and preparation methods," *International Journal of Biological Macromolecules*, vol. 169, pp. 85–94, 2021.

[10] A. Ashraf, J. Dutta, A. Farooq, M. Rafatullah, K. Pal, and G. Z. Kyzas, "Chitosan-based materials for heavy metal adsorption: Recent advancements, challenges and limitations," *Journal of Molecular Structure*, vol. 1309, p. 138225, 2024.

[11] S. Cheng, W. Grosse, F. Karrenbrock, and M. Thoennessen, "Efficiency of constructed wetlands in decontamination of water polluted by heavy metals," *Ecological engineering*, vol. 18, no. 3, pp. 317–325, 2002.

[12] F. Banat, S. Al-Asheh, and L. Abu-Aitah, "Examination of the effectiveness of physical and chemical activation of natural bentonite for the removal of heavy metal ions from aqueous solutions," *Adsorption Science & Technology*, vol. 20, no. 2, pp. 151–167, 2002.

[13] A. M. Elgarahy, K. Z. Elwakeel, S. H. Mohammad, and G. Elshoubaky, "A critical review of biosorption of dyes, heavy metals and metalloids from wastewater as an efficient and green process," *Cleaner Engineering and Technology*, vol. 4, p. 100209, 2021.

[14] W. Brack, V. Dulio, and J. Slobodnik, "The norman network and its activities on emerging environmental substances with a focus on effect-directed analysis of complex environmental contamination," *Environmental Sciences Europe*, vol. 24, pp. 1–5, 2012.

[15] J. Li, G. Luo, L. He, J. Xu, and J. Lyu, "Analytical approaches for determining chemical oxygen demand in water bodies: a review," *Critical reviews in analytical chemistry*, vol. 48, no. 1, pp. 47–65, 2018.

[16] M. Von Sperling, *Wastewater characteristics, treatment and disposal*. IWA publishing, 2007.

[17] B. Davidson and R. W. Bradshaw, "Thermal pollution of water systems," *Environmental science & technology*, vol. 1, no. 8, pp. 618–630, 1967.

[18] B. Moss, "Water pollution by agriculture," *Philosophical Transactions of the Royal Society B: Biological Sciences*, vol. 363, no. 1491, pp. 659–666, 2008.

[19] T. Deblonde, C. Cossu-Leguille, and P. Hartemann, "Emerging pollutants in wastewater: a review of the literature," *International journal of hygiene and environmental health*, vol. 214, no. 6, pp. 442–448, 2011.

[20] R. Bharti, R. Sharma *et al.*, "Effect of heavy metals: An overview," *Materials Today: Proceedings*, vol. 51, pp. 880–885, 2022.

[21] V. Renge, S. Khedkar, S. V. Pande *et al.*, "Removal of heavy metals from wastewater using low cost adsorbents: a review," *Sci. Revs. Chem. Commun*, vol. 2, no. 4, pp. 580–584, 2012.

[22] M. Barakat, "New trends in removing heavy metals from industrial wastewater," *Arabian journal of chemistry*, vol. 4, no. 4, pp. 361–377, 2011.

[23] C. Zamora-Ledezma, D. Negrete-Bolagay, F. Figueroa, E. Zamora-Ledezma, M. Ni, F. Alexis, and V. H. Guerrero, "Heavy metal water pollution: A fresh look about hazards, novel and conventional remediation methods," *Environmental Technology & Innovation*, vol. 22, p. 101504, 2021.

[24] V. Masindi and K. L. Muedi, "Environmental contamination by heavy metals," *Heavy metals*, vol. 10, no. 4, pp. 115–133, 2018.

[25] R. K. Sharma and M. Agrawal, "Biological effects of heavy metals: an overview," *Journal of environmental Biology*, vol. 26, no. 2, pp. 301–313, 2005.

[26] G. Soliman, A. ARWANA, and K. Alhakim, "Detection of lead element in cattle and sheep meat in homs governorate," *Assiut Veterinary Medical Journal*, vol. 57, no. 128, pp. 1–13, 2011.

[27] H. Sharma, N. Rawal, and B. B. Mathew, "The characteristics, toxicity and effects of cadmium," *International journal of nanotechnology and nanoscience*, vol. 3, no. 10, pp. 1–9, 2015.

[28] R. A. Bernhoft, "Mercury toxicity and treatment: a review of the literature," *Journal of environmental and public health*, vol. 2012, no. 1, p. 460508, 2012.

[29] A. W. Dobson, K. M. Erikson, and M. Aschner, "Manganese neurotoxicity," *Annals of the New York Academy of Sciences*, vol. 1012, no. 1, pp. 115–128, 2004.

[30] Y. Liu, H. Wang, Y. Cui, and N. Chen, "Removal of copper ions from wastewater: a review," *International journal of environmental research and public health*, vol. 20, no. 5, p. 3885, 2023.

[31] S. Fürtauer, *Investigation of relevant phase diagrams for high temperature solder materials: The binary systems Cu-Sn and Cu-Sb*. na, 2010.

[32] A. D. MacMahon, *Copper: a materials survey*. US Department of the Interior, Bureau of Mines, 1965, vol. 8225.

[33] F. Pizarro, M. Olivares, R. Uauy, P. Contreras, A. Rebelo, and V. Gidi, "Acute gastrointestinal effects of graded levels of copper in drinking water." *Environmental Health Perspectives*, vol. 107, no. 2, pp. 117–121, 1999.

[34] M. Pohanka, "Copper and copper nanoparticles toxicity and their impact on basic functions in the body," *Bratisl Lek Listy*, vol. 120, no. 6, pp. 397–409, 2019.

[35] M. E. Letelier, A. M. Lepe, M. Faúndez, J. Salazar, R. Marín, P. Aracena, and H. Speisky, "Possible mechanisms underlying copper-induced damage in biological membranes leading to cellular toxicity," *Chemico-biological interactions*, vol. 151, no. 2, pp. 71–82, 2005.

[36] A. HAMDOUD and A. SALHI, "Etude bibliographique sur ladsorption de quelques colorants par des bio-adsorbant." Ph.D. dissertation, Université KASDI-MERBAH Ouargla.

[37] M. E. GARRONNE, "Etude de ladsorption des covs dans les mofs par une approche complémentaire théorie-expérience," Ph.D. dissertation, Ecole Nationale Supérieure de Chimie de Montpellier, 2013.

[38] A. Ahmad, S. H. Mohd-Setapar, C. S. Chuong, A. Khatoon, W. A. Wani, R. Kumar, and M. Rafatullah, "Recent advances in new generation dye removal technologies: novel search for approaches to reprocess wastewater," *RSC advances*, vol. 5, no. 39, pp. 30 801–30 818, 2015.

[39] S. N. A. Abas, M. H. S. Ismail, M. L. Kamal, and S. Izhar, "Adsorption process of heavy metals by low-cost adsorbent: a review," *World Applied Sciences Journal*, vol. 28, no. 11, pp. 1518–1530, 2013.

[40] A. F. Belhaj, K. A. Elraies, S. M. Mahmood, N. N. Zulkifli, S. Akbari, and O. S. Hussien, "The effect of surfactant concentration, salinity, temperature, and ph on surfactant adsorption for chemical enhanced oil recovery: a review," *Journal of Petroleum Exploration and Production Technology*, vol. 10, pp. 125–137, 2020.

[41] Z. Wang, X. Wang, W. Zuo, X. Ma, and N. Li, "The influence of temperature on methane adsorption in coal: A review and statistical analysis," *Adsorption Science & Technology*, vol. 37, no. 9-10, pp. 745–763, 2019.

[42] Y. Bentahar, "Caractérisation physico-chimique des argiles marocaines: application à lad-sorption de l'arsenic et des colorants cationiques en solution aqueuse," Ph.D. dissertation, Université Côte d'Azur (ComUE), 2016.

[43] S. A. Dawood, "Development and characterization of biomass based novel adsorbent in the removal of congo red dye by adsorption," Ph.D. dissertation, Curtin University, 2013.

[44] M. Musah, Y. Azeh, J. T. Mathew, M. T. Umar, Z. Abdulhamid, and A. I. Muhammad, "Adsorption kinetics and isotherm models: a review," *CaJoST*, vol. 4, no. 1, pp. 20–26, 2022.

[45] H. H. Abdel Ghafar, G. A. Ali, O. A. Fouad, and S. A. Makhlouf, "Enhancement of adsorption efficiency of methylene blue on co3o4/sio2 nanocomposite," *Desalination and water treatment*, vol. 53, no. 11, pp. 2980–2989, 2015.

[46] K. Y. Foo and B. H. Hameed, "Insights into the modeling of adsorption isotherm systems," *Chemical engineering journal*, vol. 156, no. 1, pp. 2–10, 2010.

[47] A. Khoualdi and A. A. Medjani, "Adsorption du bleu de méthylène par le charbon actif et largile," 2016.

[48] S. Hudson and C. Smith, "Polysaccharides: chitin and chitosan: chemistry and technology of their use as structural materials," in *Biopolymers from renewable resources*. Springer, 1998, pp. 96–118.

[49] V. S. Yeul and S. S. Rayalu, "Unprecedented chitin and chitosan: A chemical overview," *Journal of Polymers and the Environment*, vol. 21, pp. 606–614, 2013.

[50] B. T. Iber, N. A. Kasan, D. Torsabo, and J. W. Omuwa, "A review of various sources of chitin and chitosan in nature," *Journal of Renewable Materials*, vol. 10, no. 4, p. 1097, 2022.

[51] C.-Y. Hsu, Y. Ajaj, Z. H. Mahmoud, G. K. Ghadir, Z. K. Alani, M. M. Hussein, S. A. Hussein, M. M. Karim, A. Al-khalidi, J. K. Abbas *et al.*, "Adsorption of heavy metal ions use chitosan/graphene nanocomposites: A review study," *Results in Chemistry*, vol. 7, p. 101332, 2024.

[52] T. J. Madera-Santana, C. H. Herrera-Méndez, and J. R. Rodríguez-Núñez, "An overview of the chemical modifications of chitosan and their advantages," *Green Materials*, vol. 6, no. 4, pp. 131–142, 2018.

[53] Q. Chen, Y. Qi, Y. Jiang, W. Quan, H. Luo, K. Wu, S. Li, and Q. Ouyang, "Progress in research of chitosan chemical modification technologies and their applications," *Marine drugs*, vol. 20, no. 8, p. 536, 2022.

[54] A. Basem, D. J. Jasim, H. S. Majdi, R. M. Mohammed, M. Ahmed, A. H. Al-Rubaye *et al.*, "Adsorption of heavy metals from wastewater by chitosan: A review," *Results in Engineering*, p. 102404, 2024.

[55] B. Arasukumar, G. Prabakaran, B. Gunalan, and M. Moovendhan, "Chemical composition, structural features, surface morphology and bioactivities of chitosan derivatives from lobster (thenus unimaculatus) shells," *International journal of biological macromolecules*, vol. 135, pp. 1237–1245, 2019.

[56] K. Alia, A. Reghioua, D. Atia, H. M. Mbuvi, Y. Moussaoui, and A. H. Jawad, "Magnetic chitosan-benzoin schiffs base/fly ash for reactive blue 19 dye removal: Characterization and parametric optimization," *Inorganic Chemistry Communications*, vol. 169, p. 112988, 2024.

[57] L. Michaelis, M. Schubert, and S. Granick, "Semiquinone radicals of the thiazines," *Journal of the American Chemical Society*, vol. 62, no. 1, pp. 204–211, 1940.

[58] D. A. M. Osman and M. A. Mustafa, "Synthesis and characterization of zinc oxide nanoparticles using zinc acetate dihydrate and sodium hydroxide," *J. Nanosci. Nanoeng*, vol. 1, no. 4, pp. 248–251, 2015.

[59] P. O. Oladoye, O. M. Olowe, and M. D. Asemoloye, "Phytoremediation technology and food security impacts of heavy metal contaminated soils: A review of literature," *Chemosphere*, vol. 288, p. 132555, 2022.

[60] J. Fronczyk, K. Kuśmierek, and A. Świątkowski, "Reactive red 120 dye removal from water systems using natural minerals: Batch adsorption approach," *Water, Air, & Soil Pollution*, vol. 236, no. 2, p. 138, 2025.

[61] A. S. Abdulhameed, S. Abdullah, A. A. Al-Masud, M. Abualhaija, and S. Algburi, "Chitosan polymer-loaded chemically treated mango (mangifera indica l.) peel biomass for the adsorption of safranin o dye using box-behnken design," *Biomass Conversion and Biorefinery*, pp. 1–16, 2025.

[62] J. Li, B. Jiang, Y. Liu, C. Qiu, J. Hu, G. Qian, W. Guo, and H. H. Ngo, "Preparation and adsorption properties of magnetic chitosan composite adsorbent for cu2+ removal," *Journal of Cleaner Production*, vol. 158, pp. 51–58, 2017.

[63] A. Vinu, T. Mori, and K. Ariga, "New families of mesoporous materials," *Science and technology of Advanced materials*, vol. 7, no. 8, pp. 753–771, 2006.

[64] A. S. Abdulhameed, S. Abdullah, A. A. Altamimi, M. Abualhaija, and S. Algburi, "Development of a schiff base-chitosan-vanillin/hydroxyapatite composite for effective brilliant green dye removal: Characterization, adsorption modeling, and cost analysis," *International Journal of Biological Macromolecules*, p. 143140, 2025.

[65] Z. Zhang and H. Zheng, "Optimization for decolorization of azo dye acid green 20 by ultrasound and h2o2 using response surface methodology," *Journal of hazardous materials*, vol. 172, no. 2-3, pp. 1388–1393, 2009.

[66] J. V. Oliveira, M. Alves, and J. Costa, "Biochemical methane potential of brewery by-products," *Clean Technologies and Environmental Policy*, vol. 20, no. 2, pp. 435–440, 2018.

[67] S. Lal, S. Arora, V. Kumar, S. Rani, C. Sharma, and P. Kumar, "Thermal and biological studies of schiff bases of chitosan derived from heteroaryl aldehydes," *Journal of Thermal Analysis and Calorimetry*, vol. 132, pp. 1707–1716, 2018.

[68] F. Han, A. S. Hessen, A. Amari, N. Elboughdiri, and S. Zahmatkesh, "Heavy metal (cu2+) removal from wastewater by metal-organic framework composite adsorbent: Simulation-based-artificial neural network and response surface methodology," *Environmental Research*, vol. 245, p. 117972, 2024.

[69] D. Zhao, H. Wang, Z. Wang, and S. Lu, "Understanding competitive cu2+ and zn2+ adsorption onto functionalized cellulose fiber via experimental and theoretical approach," *International Journal of Biological Macromolecules*, vol. 273, p. 132782, 2024.

[70] S. Varshney, P. Jain, J. K. Arora, and S. Srivastava, "Process development for the removal of toxic metals by functionalized wood pulp: kinetic, thermodynamic, and computational modeling approach," *Clean Technologies and Environmental Policy*, vol. 18, pp. 2613–2623, 2016.

[71] S.-Z. Xu, T. Zhao, Q. Chen, X.-G. Liang, and Z.-Y. Guo, "State functions/quantities in thermodynamics and heat transfer," *Fundamental Research*, vol. 2, no. 1, pp. 101–107, 2022.

[72] M. M. Kaci, I. Akkari, M. Pazos, F. Atmani, and H. Akkari, "Recent trends in remediating basic red 46 dye as a persistent pollutant from water bodies using promising adsorbents: a review," *Clean Technologies and Environmental Policy*, pp. 1–16, 2024.

[73] S. Lagergren, "Zur theorie der sogenannten adsorption geloster stoffe," *Kungliga svenska vetenskapsakademiens. Handlingar*, vol. 24, pp. 1–39, 1898.

[74] Y.-S. Ho and G. McKay, "Sorption of dye from aqueous solution by peat," *Chemical engineering journal*, vol. 70, no. 2, pp. 115–124, 1998.

[75] M. C. Vishwakarma, H. K. Joshi, P. Tiwari, N. S. Bhandari, and S. K. Joshi, "Thermodynamic, kinetic, and equilibrium studies of cu (ii), cd (ii), ni (ii), and pb (ii) ion biosorption onto treated ageratum conyzoid biomass," *International Journal of Biological Macromolecules*, vol. 274, p. 133001, 2024.

[76] S. Chkirida, N. Zari, R. Achour, A. e. k. Qaiss, and R. Bouhfid, "Efficient hybrid bionanocomposites based on iron-modified tio 2 for dye degradation via an adsorption-photocatalysis synergy under uv-visible irradiations," *Environmental Science and Pollution Research*, vol. 28, pp. 14 018–14 027, 2021.

[77] I. Langmuir, "The adsorption of gases on plane surfaces of glass, mica and platinum." *Journal of the American Chemical society*, vol. 40, no. 9, pp. 1361–1403, 1918.

[78] H. Freundlich, "Über die adsorption in lösungen," *Zeitschrift für physikalische Chemie*, vol. 57, no. 1, pp. 385–470, 1907.

[79] M. Tempkin, V. Pyzhev *et al.*, "Kinetics of ammonia synthesis on promoted iron catalyst," *Acta Phys. Chim. USSR*, vol. 12, no. 1, p. 327, 1940.

[80] S. Azizian and M. Bagheri, "Enhanced adsorption of cu2+ from aqueous solution by ag doped nano-structured zno," *Journal of Molecular Liquids*, vol. 196, pp. 198–203, 2014.

[81] W. W. Ngah and S. Fatinathan, "Adsorption of cu (ii) ions in aqueous solution using chitosan beads, chitosan–gla beads and chitosan–alginate beads," *Chemical Engineering Journal*, vol. 143, no. 1-3, pp. 62–72, 2008.

[82] Q. Liu, B. Yang, L. Zhang, and R. Huang, "Simultaneous adsorption of aniline and cu2+ from aqueous solution using activated carbon/chitosan composite," *Desalination and Water Treatment*, vol. 55, no. 2, pp. 410–419, 2015.

[83] M. Monier, "Adsorption of hg2+, cu2+ and zn2+ ions from aqueous solution using formaldehyde cross-linked modified chitosan–thioglyceraldehyde schiff's base," *International journal of biological macromolecules*, vol. 50, no. 3, pp. 773–781, 2012.

[84] M. M. Rahman, M. S. Yeasmin, M. J. Uddin, M. Hasan, M. A. A. Shaikh, M. S. Rahman, and M. Maniruzzaman, "Simultaneous abatement of ni2+ and cu2+ effectually from industrial wastewater by a low cost natural clay-chitosan nanocomposite filter: Synthesis, characterization and fixed bed column adsorption study," *Environmental Nanotechnology, Monitoring & Management*, vol. 20, p. 100797, 2023.

[85] L. Zhao and H. Mitomo, "Adsorption of heavy metal ions from aqueous solution onto chitosan entrapped cm-cellulose hydrogels synthesized by irradiation," *Journal of Applied Polymer Science*, vol. 110, no. 3, pp. 1388–1395, 2008.

[86] J. Xiong, Y. He, X. Cui, and L. Liu, "Preparation of amino-bagasse/metakaolin based geopolymer hybrid microsphere as a low-cost and effective adsorbent for cu (())," *Journal of Environmental Chemical Engineering*, vol. 11, no. 5, p. 110954, 2023.

[87] X. Wang, W. Cai, Y. Lin, G. Wang, and C. Liang, "Mass production of micro/nanostructured porous zno plates and their strong structurally enhanced and selective adsorption performance for environmental remediation," *Journal of Materials Chemistry*, vol. 20, no. 39, pp. 8582–8590, 2010.